STRESS ANALYSIS OF BELLOWS FOR THE HNPF INTERMEDIATE HEAT EXCHANGER

AEC Research and Development Report

ATOMICS INTERNATIONAL
A DIVISION OF NORTH AMERICAN AVIATION, INC.

NAA-SR-4534
REACTOR TECHNOLOGY
59 PAGES

STRESS ANALYSIS OF BELLOWS FOR THE HNPF INTERMEDIATE HEAT EXCHANGER

By

R. CHIPMAN
R. GALANTINE
J. SUSNIR

ATOMICS INTERNATIONAL

A DIVISION OF NORTH AMERICAN AVIATION, INC.
P.O. BOX 309 CANOGA PARK, CALIFORNIA

CONTRACT: AT(11-1)-GEN-8
ISSUED: APR 15 1962

DISTRIBUTION

This report has been distributed according to the category "Reactor Technology" as given in "Standard Distribution Lists for Unclassified Scientific and Technical Reports" TID-4500 (16^{th} Ed.), December 15, 1960. A total of 650 copies was printed.

CONTENTS

TABLES

FIGURES

ABSTRACT

A combined theoretical and experimental stress analysis was performed on a bellows to determine if it was suitable for use in absorbing the differential expansion between the shell and tubes of the intermediate heat exchanger for the Hallam Nuclear Power Facility (HNPF). The following modes of deformation were imposed, singly and in combination, upon a prototype bellows at room temperature: axial deflection, lateral deflection, angular rotation, torsional rotation, and pressurization. Good agreement was obtained between predicted and observed strains. All subsequent tests were performed with sodium at 75 psig and 1000°F inside the bellows. During the first series of these tests, which simulated the cycling effects of 20 years of normal reactor operation, negligible damage occurred in the bellows. The second series of tests, with sodium at 75 psig and 1000°F, showed that the bellows could withstand the large axial deflections which might occur during abnormal conditions involving failure of a pump in either the primary or secondary cooling system. In the final series of tests, the axial deflection stroke was gradually increased in a deliberate attempt to induce failure in the bellows. When the stroke was increased to approximately 30 times that expected during normal operation, a reproducible signal was obtained indicating that sodium had leaked through the inner ply of the double-ply wall. Even at that time, there was no leakage of sodium through the outer ply and the bellows still remained functional. It was concluded that the bellows is well suited for application in the HNPF intermediate heat exchanger.

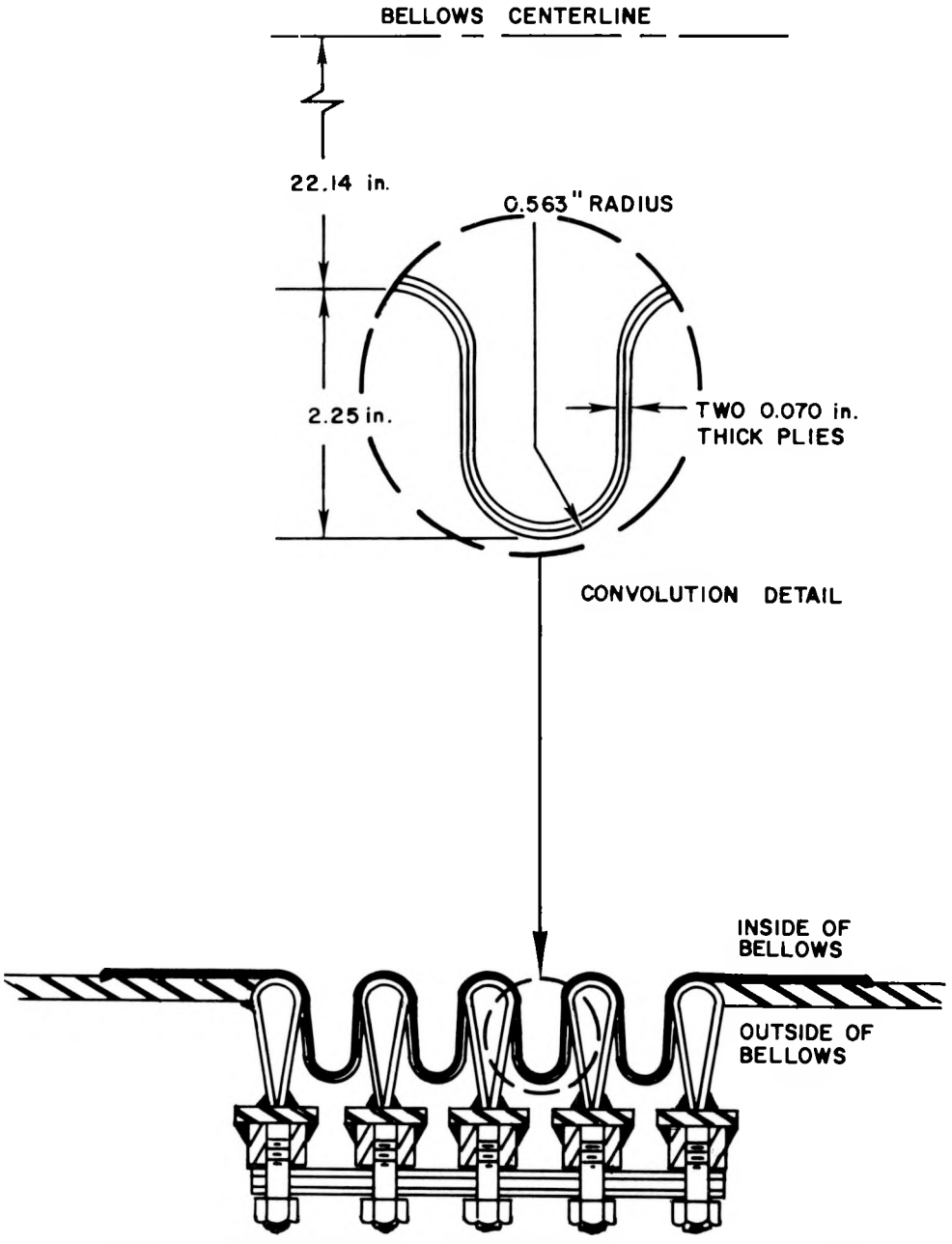

Figure 2. Bellows for Intermediate Heat Exchanger

20 years of normal reactor service. The third phase of testing was to determine the effect of abnormal conditions developed by a failure of a pump in either the primary or secondary cooling system of the HNPF. The fourth and final phase of testing was to deliberately induce failure of the bellows by gradually increasing the axial-deflection-stroke magnitude. The first phase of testing was to be performed at room temperature without sodium; all subsequent tests were to be performed with sodium inside the bellows, at pressures up to 75 psig and temperatures up to 1000°F. Based upon these tests it should then be possible: (a) to predict how the bellows would behave under designated loading conditions, (b) to ascertain whether the bellows would meet the operational requirements, and (c) to gain further insight as to the extreme conditions required to cause failure of the bellows and the mode of failure which might then ensue.

This report is intended to describe the method by which the expected loads and deformations were computed, the fixture used to impose the various modes of loading upon the bellows, the procedure followed and the results obtained during testing of the bellows at both room and elevated temperatures, and the stress analysis of the bellows including derivation of equations.

The following terms will be used to describe the movements of the bellows caused by forces or moments (see accompanying sketch, Figure 3).

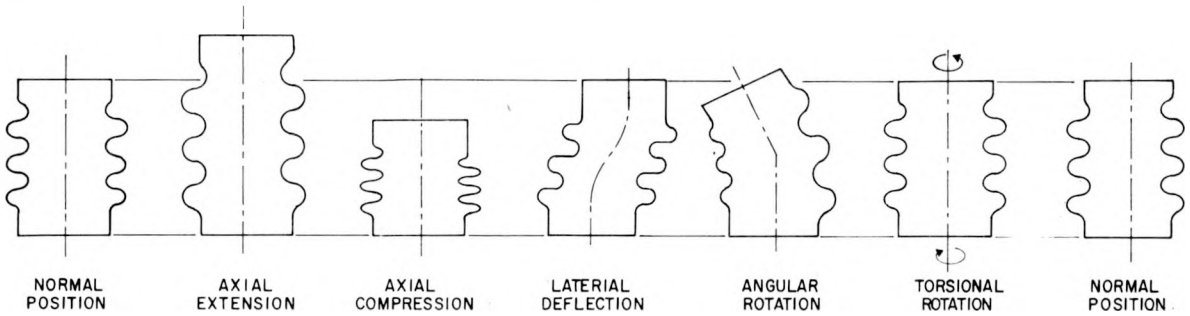

Figure 3. Schematic Representation of Bellows Movements

Axial deflection is movement of the bellows parallel to its longitudinal axis. This deflection may consist of either axial compression or axial extension, depending upon whether the bellows is being shortened or lengthened, and is caused by an axial force.

Lateral deflection is the relative displacement of the two ends of a bellows perpendicular to its longitudinal axis while the ends are maintained parallel. This lateral movement is caused by a side force.

Angular rotation is the bending of the longitudinal axis of a bellows from its initial straight line position. This tilting of the end faces of a bellows is caused by a bending moment.

Torsional rotation is the rotation of a bellows about its longitudinal axis. This axial twisting of the bellows is caused by a torsional moment.

Another term which will be used in this report to describe the cumulative effect on the bellows of various loads and deformation is that of damage factor. Damage factor is the fraction of total expected life of a component which has been expended because of cumulative cyclic strain. This factor sums the effect of operation at various strain levels, so that one can estimate the remaining number of cycles to failure at different strain levels. When the damage factor totals 1.0, theoretically the component will fail. For example, if a component has been exposed to cyclic strain conditions resulting in a damage factor of 0.8, then the remaining number of cycles at a new strain level should be (1-0.8) or 0.2 of the total number of cycles which an unstrained component could endure at the new strain level.

II. TEST LOADS AND DEFORMATIONS

Service loads and deflections imposed on the bellows in the intended application are a function of the relative expansion between tubes and shell, piping loads, internal pressure, the stiffness of the bellows relative to the support structure, and the supporting-guide clearances. It was necessary to formulate the bellows test program before the intermediate-heat-exchanger design and the associated piping layout were completed. Design values for the internal pressure and axial deflections of the bellows had been established; but the side force, torque, and end moment that would be imposed on the bellows had not. Therefore, conservative (larger than expected) estimates were made of the latter values. The support structure was included in the heat exchanger design to limit the side deflection, axial deflection, and end rotation of the bellows. Conservative (larger than expected) estimates also were made of the movements which the structure would permit to allow for possible deviations from specified manufacturing tolerances.

As an example of the conservative nature of the above assumptions, the limiting axial torque (at room temperature) was established as 75,000 ft-lb; calculations incorporating present design piping loads indicate that this value will be 20,300 ft-lb. Thus, this particular load is conservative by a factor of 3.7. Similar conservatism was used in deriving all the limiting values, with the exception of those for internal pressure and axial deflection, as these two limits were known with reasonable certainty at the time the test program was formulated. The internal pressure and axial deflection were adjusted for temperature effects; these adjustments were made by increasing the pressure value and deflections by the ratio of the allowable stress for 304 stainless steel at room temperature to that at design temperature, using data from the ASME Unfired Pressure Vessel Code. As an example of such an adjustment for temperature effects, the limiting internal pressure for the combined load test was calculated as follows:

Design Temperature	= 1000°F
Design Pressure	= 100 psi
Material	= Type 304 stainless steel
Allowable Stress at Room Temperature	= 18,750 psi
Allowable Stress at 1000°F	= 8,800 psi
Room Temperature Test Pressure	= 18,750/8,800 x 100 = 210 psi

A summary of the design loads and deformations which were established for the test program is given in Table I. For the last three types of loading, both loads and deflections are given because the bellows is limited in deflection by the restraining framework; therefore, loads were to be imposed until either the specified value of load or deflection was reached, regardless of which occurred first.

TABLE I

DESIGN LOADS AND DEFORMATIONS FOR BELLOWS TEST PROGRAM

Load			Deformation		
Type	At Room Temperature	At 1000°F	Type	At Room Temperature	At 1000°F
Axial Force	No Limit	No Limit	Axial Deflection	0.85 in.	0.35 in.
Internal Pressure	320 psig (Proof Test) 210 psig (Combined Tests)	75 psig	Convolution Expansion	*	*
Bending Moment	185,000 lb-ft	---	Angular Rotation	0.10°	---
Side Force	20,000 lb	---	Lateral Deflection	0.10 in.	---
Torsional Moment	75,000 lb-ft	---	Torsional Rotation	0.10°	---

*Material must remain intact and not fracture.

III. TEST APPARATUS

A. PRESSURE VESSEL AND LOADING FRAMEWORK

In order to perform the test program, it was necessary to provide a means for pressurizing the bellows and for applying the required loads. A pressure vessel (shown in Figures 4 and 5) was fabricated by welding flanged and dished

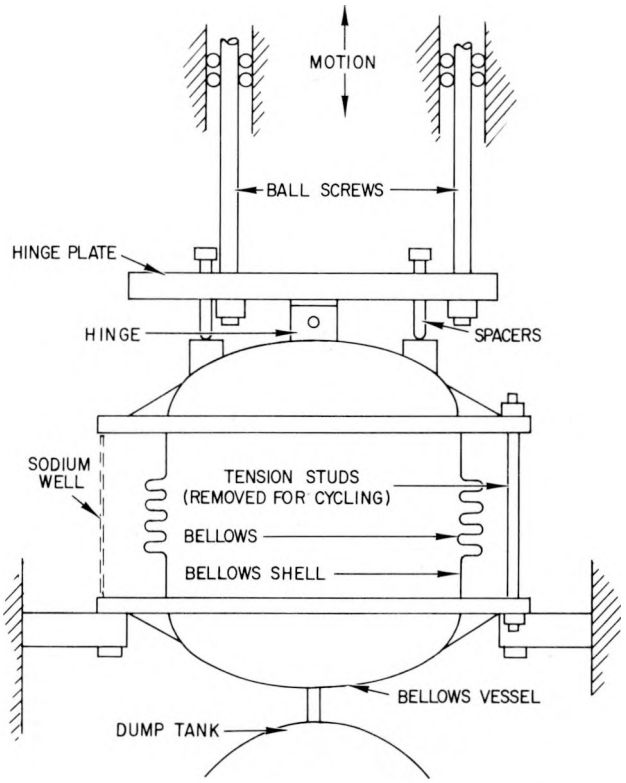

Figure 4. Test Fixture for Bellow Tests

heads to a 9/16-in.-thick by 5-7/8-in.-long shell at each end of the 44-in.-diameter bellows. Two 58-in.-diameter by 2-in.-thick flanges were welded to the pressure vessel and served to position the bellows in the test fixture. The test fixture used to apply the loads was an adjustable structural framework built around four cylindrical columns, within which the bellows was positioned so that its axis of symmetry was vertical. Each column was made from a 12-ft-long section of cold-drawn, 6-in. steel pipe, threaded over 11 ft of its length, with a 17-in.-diameter by 2-in.-thick flange welded to the bottom end. The columns were bolted through these flanges to four adjacent 25,000-lb tie-points in an existing structural floor to form a 4-ft-square by 12-ft-high framework. Each column

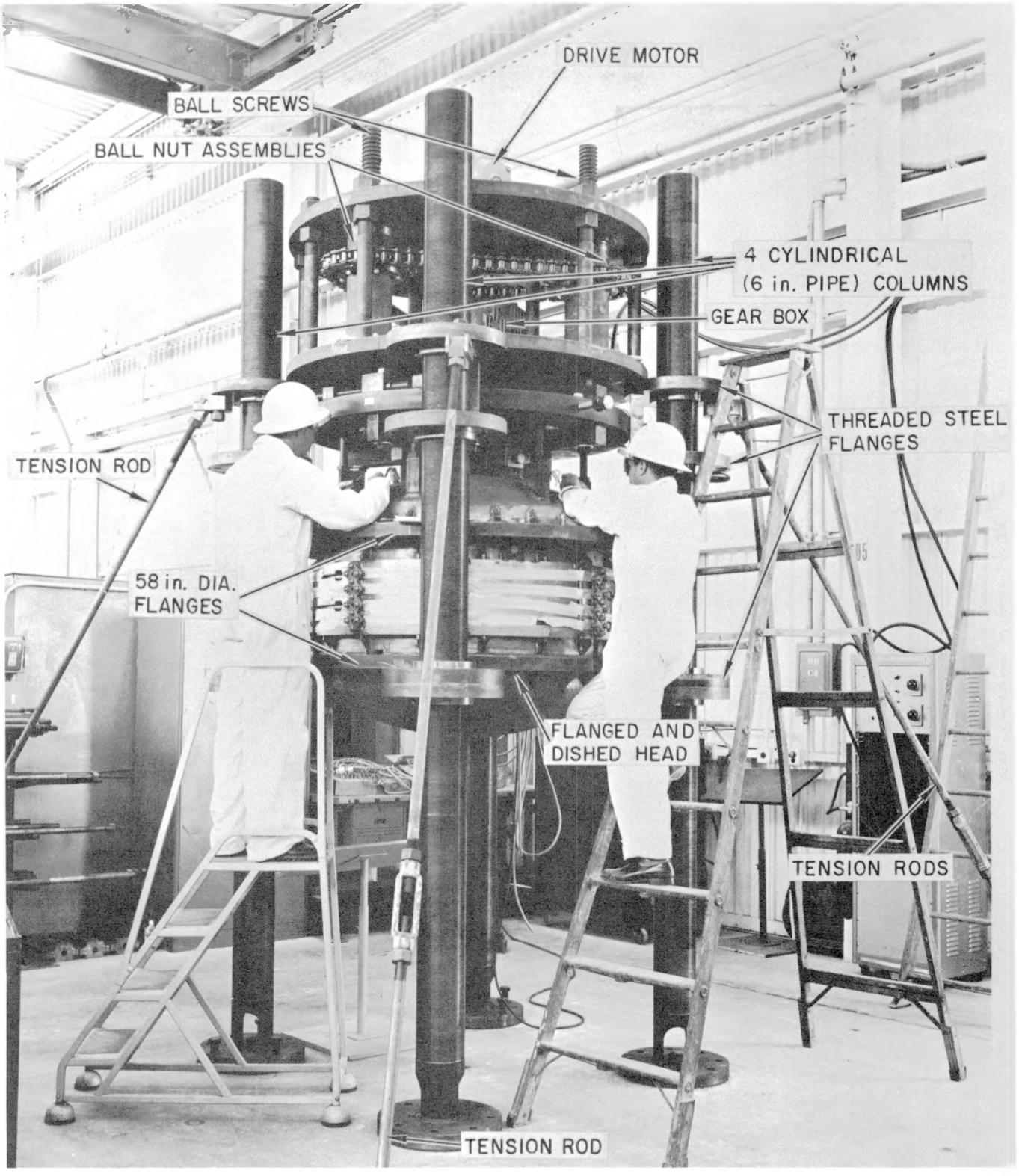

Figure 5. Testing Framework and Bellows Vessel

was braced by diagonal tension rods attached to 5,000-lb tie points in the floor. To position the HNPF test bellows within this structure, it was necessary to remove one column, place the bellows in the framework, and then replace the column.

Sixteen threaded steel flanges (17-in. diameter by 2-in. thick) were run onto the columns to provide support and attachment points for the bellows and related test fixtures; these flanges were secured by locking nuts. The tension rods between the uppermost flanges and outer tie-points in the floor served to stabilize the columns.

The axial drive-mechanism was comprised of three ball-screw assemblies, a high-reduction gear box, and a reversing electric motor. The ball screws did not rotate, but were moved up and down by chain-driven ball-nut assemblies. These screws had a maximum vertical travel of 30 in. at a rate of $\sim$12 in./min. The amount of axial deflection during a cycle was controlled by varying the position of micro-switches; upon reaching either top or bottom limit of travel, the drive motor was reversed by the switches. Drive-mechanism controls permitted either manual or automatic operation of axial-deflection cycling of the bellows.

The cycling mechanism was supported by a 58-in.-diameter by 2-in.-thick steel plate, which was bolted to the uppermost column flanges. The ball screws protruded through this plate and bolted into a 52-in.-diameter by 3-in.-thick loading ring, which moved vertically inside the column framework.

A special hinge-plate (Figures 4 and 6) was devised for lateral deflection, angular rotation, and torsional rotation tests. The pressure vessel was attached to the plate at the hinge and the bottom flange of the vessel was bolted to column flanges to provide necessary restraint for the bottom of the unit. Cross members, which were attached to the hinge-plate, supported the plate in the plane of the loading ring (see Figure 6). Torsional rotation of the bellows was accomplished by reacting between the loading ring and the cross members, and lateral deflection by reacting between the ring and the hinge-plate. Angular rotation was accomplished by reacting between the top of the bellows vessel and the loading ring, causing rotation about the hinge.

The framework had an axial-load capacity of 115,000 lb, for reaction against the columns (although reaction against the floor was limited to 100,000 lb). By using sixteen 1-in.-diameter tension rods between flanges on the bellows vessel,

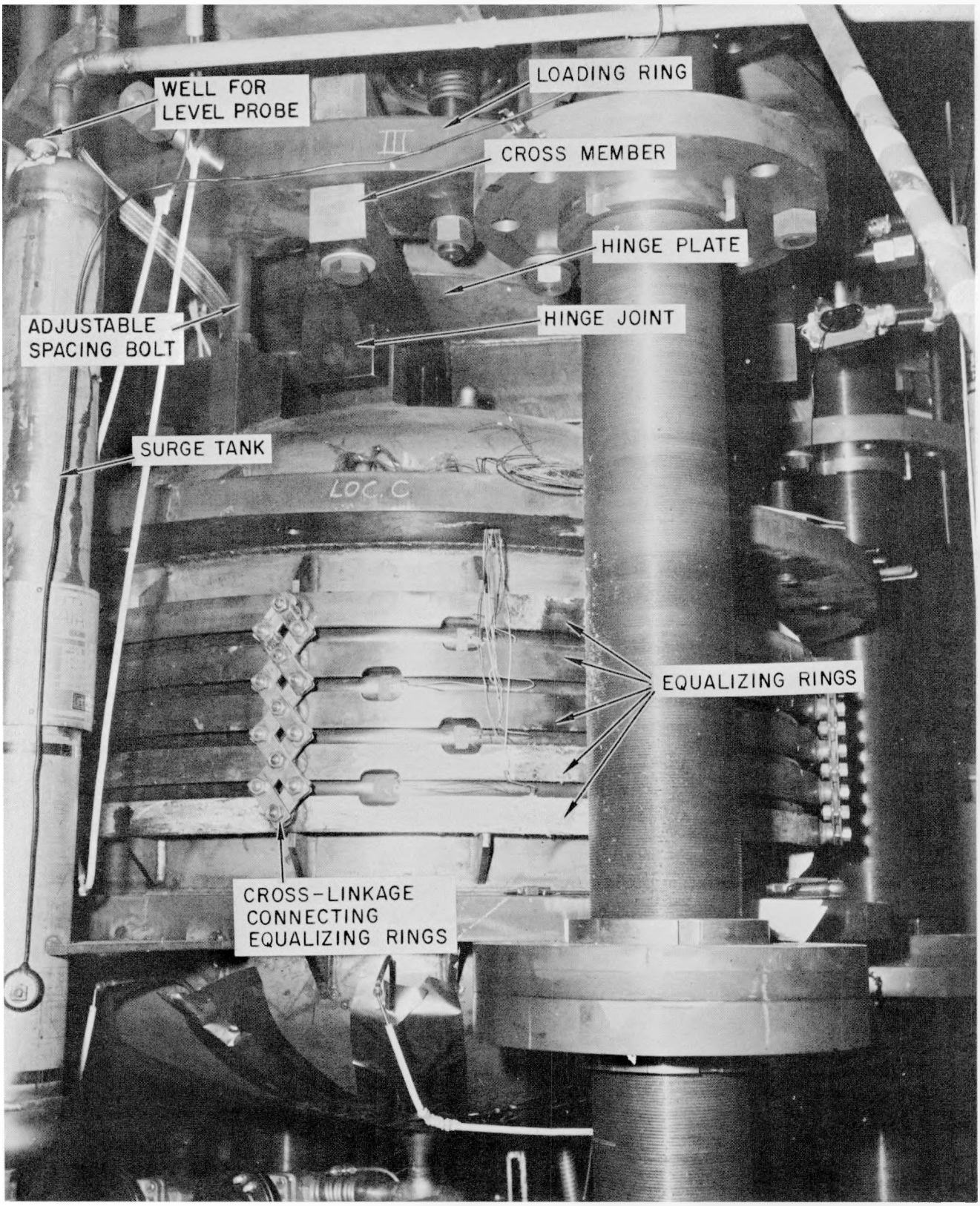

Figure 6. Bellows Vessel and Loading Fixture Details

it was possible to pressurize the unit to 325 psig, which corresponded to an axial force of 500,000 lb.

Lateral forces were reacted by the columns through large cam-following bearings; this was done to protect the ball screws from bending loads. The bearings were bolted horizontally into the loading ring at points opposite each column. A heavy, slotted block was attached between the two top flanges of each column so that the bearing moved vertically in the slot. Axial travel was limited to one inch above and below the free position of the bellows to avoid accidental overstressing of the bellows.

B. SODIUM SYSTEM

A system was required for storing, heating, and handling sodium at temperatures to 1000°F and pressures to 80 psig. This system was comprised of a 230-gal storage tank, the bellows vessel itself, a surge tank, distribution piping, valves, and the associated instrumentation and controls. Heating was performed by tubular electric-resistance units, which were attached to all vessels and piping; six 1500-watt heaters were required to bring the sodium in the bellows vessel up to testing temperatures. All welds were X-rayed, and prior to filling with sodium, the entire system was leak checked with a mass-spectrometer leak detector using helium.

The storage tank was filled with molten sodium by gravity flow directly from supply barrels. Transferring of sodium from the storage tank to the test vessel was done by pressurizing the storage tank with nitrogen. At the conclusion of each test, sodium was transferred back from the bellows to the storage tank by gravity flow.

Two techniques were devised for detecting leaks in the bellows; both techniques utilized the space between the two plies. In the first method, helium gas at 5 psig was introduced between the plies and the resultant gas pressure was measured; it was reasoned that changes in pressure would indicate leaking in one ply or the other (depending upon the relative pressure levels in the vessel, between the plies, and outside the vessel). An experiment, which was conducted during final assembly of the bellows, proved that helium gas would pass between the plies, despite the fact the plies were formed conjointly and appeared to be in intimate contact with each other.

The second leak-detection technique incorporated a well, which was connected to a coupling through the outer ply only. A spark-plug electrode was extended to within a fraction of an inch of the bottom of the well; the other terminal was connected to the well. An alarm bell was wired in series with the spark plug and dry-cell batteries. If a leak occurred in the inner ply, sodium would fill the space between plies, then overflow into the well, close the circuit, and the bell would ring.

A feature of the system which provided secondary containment for the sodium was a steel well at the floor level. Curved plates nested in the well and provided containment for thermal insulation (expanded mica), with which the sodium system and bellows vessel were completely covered during testing at high temperatures. The bellows was wrapped with aluminum foil to prevent the granular insulating material from working between the convolutions and the equalizing rings during axial cycling. To prevent overheating, it was necessary to cool the flanges which supported the bellows vessel. Insulation blockouts were provided underneath the flanges, and tubes extended from these chambers upward through flange holes and insulation. Cooling air circulated through the tubes by natural convection and reduced the temperature of the column and flanges.

C. INSTRUMENTATION

It was of prime importance to determine the magnitudes of strains at critical locations on the bellows during various loading and deformation tests. Therefore, electric-resistance strain gages were installed at such points, insofar as they were accessible.

Thirty-eight strain gages were installed inside the bellows prior to fabrication of the pressure vessel (of which the bellows was a part). These gages were located along three axial runs, spaced at 120° around the circumference of the unit, as shown in Figure 7. All gage installations inside the tank were made waterproof for internal pressurization tests. Lead wires were brought out the top of the vessel through three special plugs. Twelve strain gages were installed outside the bellows on convolution apexes, with four gages along each of the three axial runs; later in the testing program one strain rosette was installed along each run at a convolution apex. Strain gages also were installed on the drive-mechanism ball screws for the purpose of determining axial loads. A 50-channel recorder was used to record strain data for all room-temperature tests.

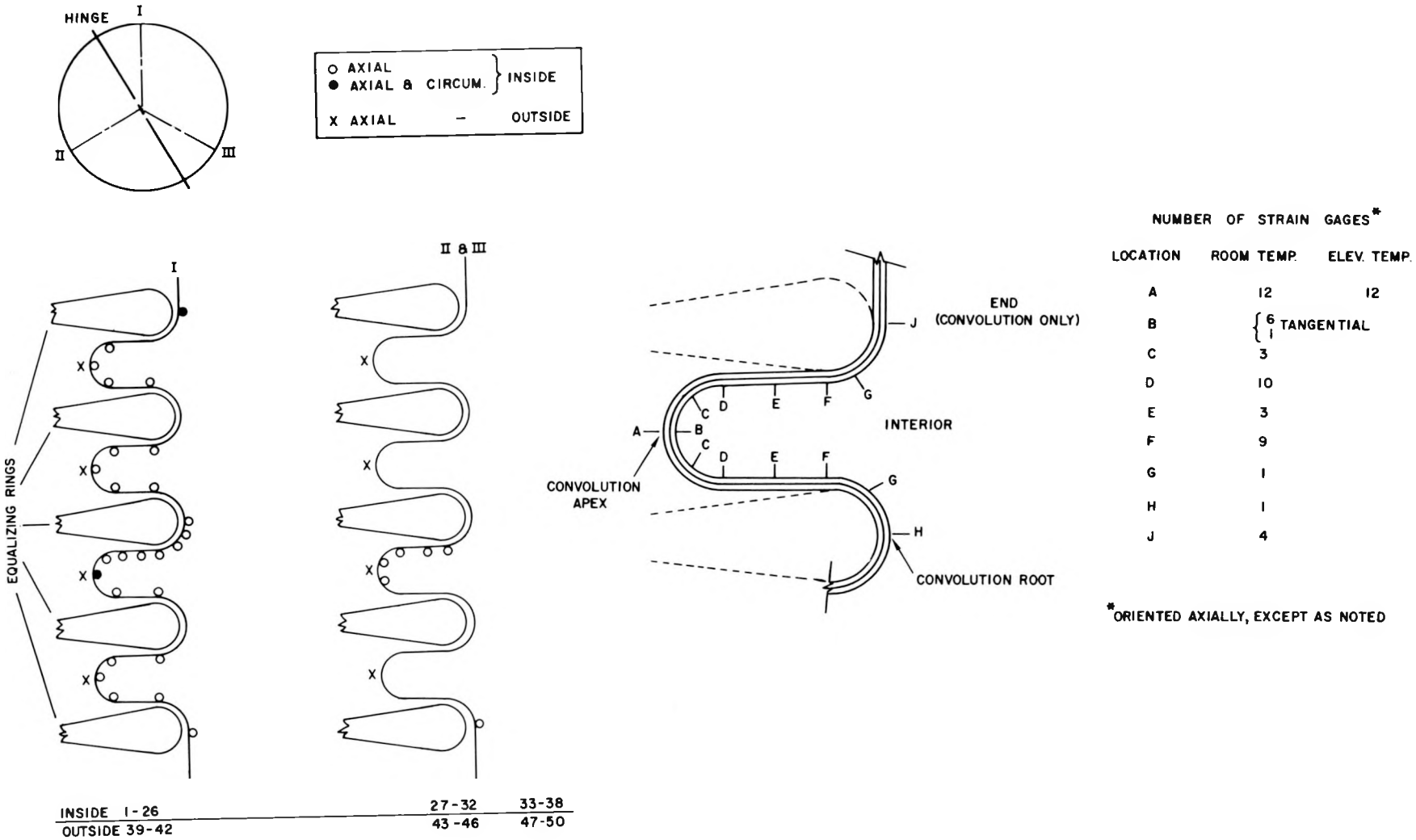

LOCATION	NUMBER OF STRAIN GAGES* ROOM TEMP.	ELEV. TEMP.
A	12	12
B	6 TANGENTIAL, 1	
C	3	
D	10	
E	3	
F	9	
G	1	
H	1	
J	4	

*ORIENTED AXIALLY, EXCEPT AS NOTED

Figure 7. Strain-Gage Locations

Prior to testing with sodium inside the bellows, all lead wires inside the unit and as much of each gage installation as possible were removed. This was done to minimize the addition of foreign matter to the sodium. The original room-temperature gages outside the unit were replaced by other gages which were suited for high-temperature service. A 40-channel recorder was used to record strain and temperature data for the elevated-temperature tests.

Hydraulic rams, calibrated in terms of pressure, were used to twist, tilt, and laterally deflect the top of the bellows with relation to the bottom. Resulting deflections were measured by dial extensometers.

An inductance-type probe was used to locate the level of sodium in the test vessel. The probe was inserted into a well in the surge tank for these measurements.

IV. ROOM TEMPERATURE TESTING PROGRAM

A. TENSILE STRESS-STRAIN TESTS

Prior to starting the regular testing program, tensile coupons were machined from the same sheets from which the bellows had been fabricated. Coupons were taken from both inner and outer ply material, and with axes both parallel and transverse to the direction of rolling. Tensile tests were conducted at room temperature and 1000°F. There was no significant difference in properties of the inner and outer plies, and the following values were obtained:

Property	Room Temperature	1000°F
Ultimate Strength (psi)	88,700	57,000
Modulus of Elasticity (psi)	28×10^6	21×10^6
Yield Strength (psi)	42,000	24,000

B. POSITIONING THE BELLOWS FOR TESTING

It was necessary to determine the free, or equilibrium, position of the bellows experimentally as the manufacturer had compressed the unit and attached restraining straps on the outside of the bellows prior to shipping. These straps were removed only after assembly of the vessel was completed and the bellows was attached to the test fixture by the hinge on the upper head. The vessel was alternately suspended by the hinge, and then brought to rest on the column flanges and the hinge was detached. The respective elongation and shortening of the bellows were plotted versus known tension and compression forces, which were derived from the weights of top and bottom portions of the vessel. The free position of the unit was then determined by interpolation to be ~ 1/2 inch extended from the shipping position. Throughout the remainder of the testing program, deformations of the bellows were referred to this free position.

The top of the bellows was maintained in a plane parallel to that of the loading ring by adjustable spacing-bolts (see Figure 6), except during angular rotation (end-tilting) tests. This parallelism was required to assure uniform distribution around the bellows of deformation resulting from extending or compressing the unit.

C. AXIAL DEFLECTION TESTS

Axial deflection tests were conducted on the bellows first, as this is the deformation mode for which the unit was primarily designed. The spring constant was determined by supporting the bellows vessel with the hinge and elongating the unit with a double-acting hydraulic cylinder; the cylinder was attached at the center of the bottom head of the vessel and reacted against the structural floor. Load and extension were measured and a spring constant of 29,000 ± 2,300 lb/in. was derived from these data.

The lower flange of the pressure vessel was then bolted to the testing framework, and the unit was extended to 0.58-in. (using the axial drive mechanism) in successive steps of increasing magnitude. The load was removed after each step, and the bellows was returned to its original free position. At each loading step and at each return to zero, strain and extension data were recorded. Strain vs extension data are plotted in Figure 8, where vertical lines indicate the range of data and point symbols represent the average of data at each type of location. Inside surfaces at convolution apexes (locations B) were the most highly strained elements in the unit. When the bellows was returned to its original free position, strain readings returned to approximately zero, indicating that no significant inelastic deformation had occurred in the unit.

Although drive-mechanism ball screws were instrumented with strain gages, readings during extension testing were too small to provide an accurate basis for calculating axial loads on the bellows.

For purpose of comparison with the measured values, strains in the bellows due to extension were derived theoretically. An elastic analysis was used, and it was assumed that no friction or other interaction effects occurred between the two plies. The following equation* for maximum strain assumes that each convolution is restrained from rotating at the apex:

$$\epsilon_{max} = \frac{t\, d\, C_1}{4S} \qquad \ldots (1)$$

*See Appendix A for derivation; Equation 1 corresponds to Equation 9 in the Appendix. See Page 53 for Nomenclature.

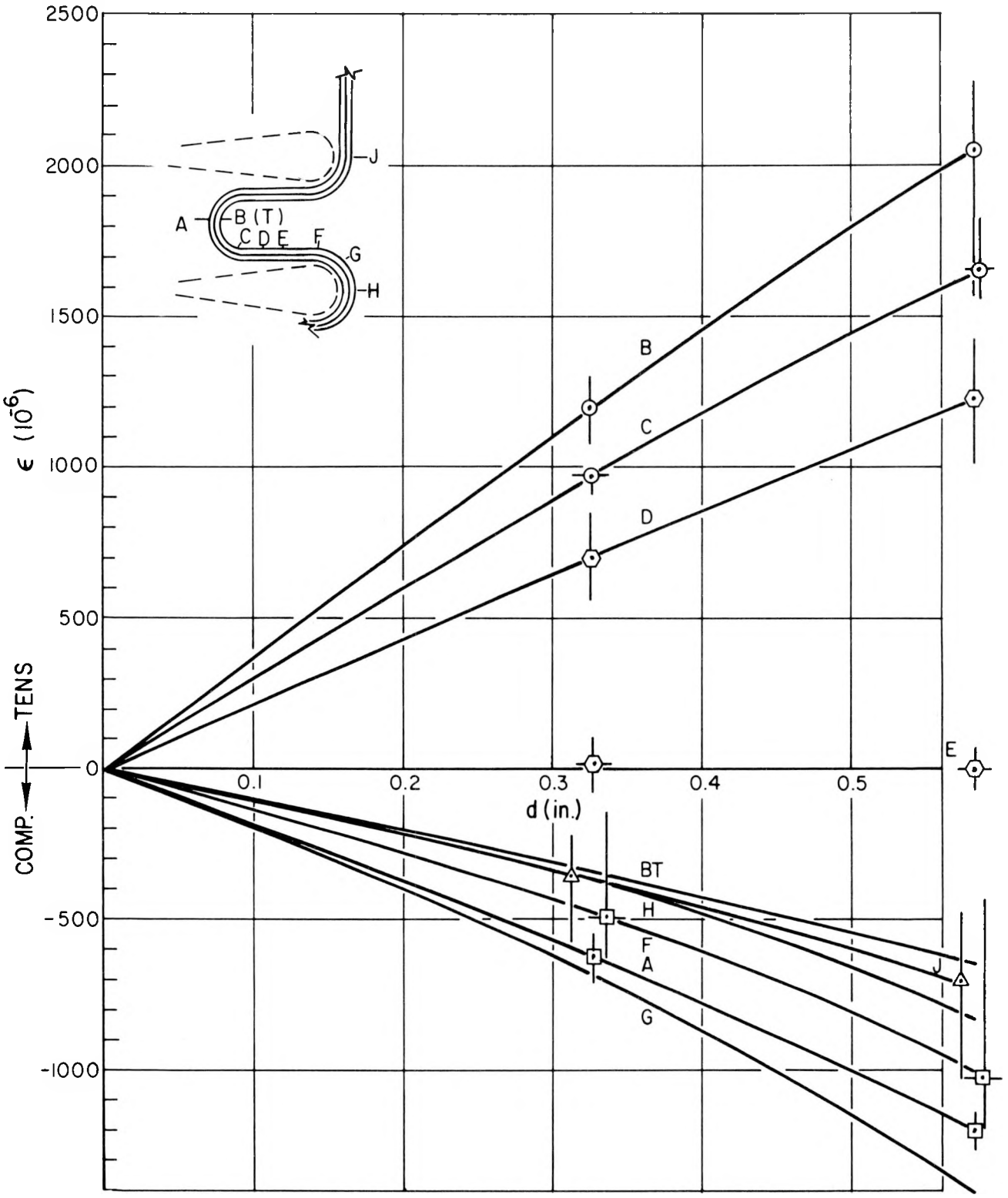

Figure 8. Strain vs Axial Deflection of Bellows at Room Temperature

Substituting appropriate constants for the test bellows, the strain is obtained as a function of axial displacement, d, of the bellows.

$$\epsilon_{max} = 0.00296\ d \quad (\text{in./in.})$$

or

$$\epsilon_{max} = 2{,}960\ d \quad (\mu\text{in./in.})$$

Comparison of the theoretical and test curves (Figure 9) for extension in the elastic region indicates that the measured strains are approximately 25% higher than theoretical values. The greatest portion of this difference is probably due to the shear forces resulting from friction developed between the two plies; this would result in higher moments acting at the various sections.

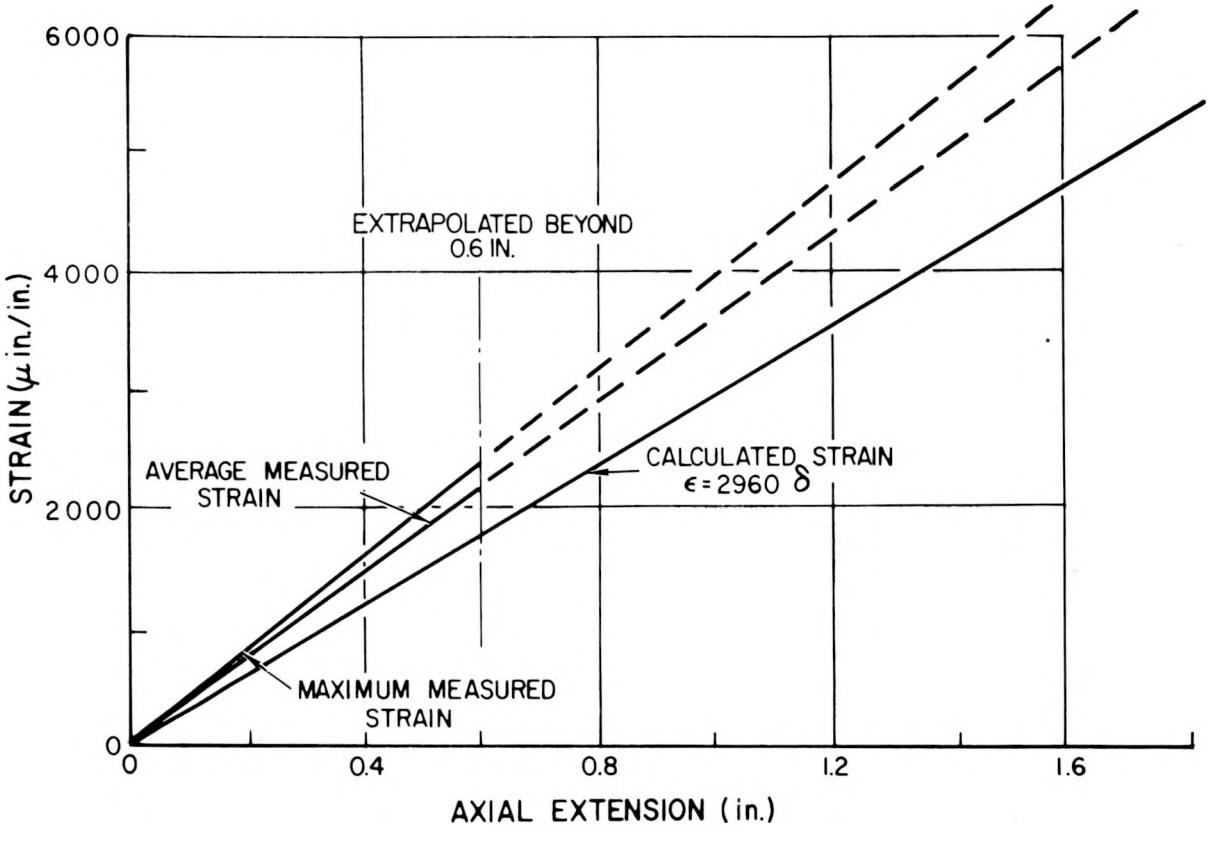

Figure 9. Comparison of Theoretical and Experimental Data for Axial Extension

D. INTERNAL PRESSURIZATION TESTS

The bellows vessel was pressurized with water to a maximum of 325 psig. Again, loading was done in steps; strain data were recorded at pressure levels of approximately 100, 200, and 325 psig and at each subsequent return to zero conditions. Many of the strain gages inside the vessel shorted-out at pressures above 150 psig; however, upon draining the water and blowing warm air into the vessel, the majority of these gages became operative again. Typical data from pressurization tests are presented in Figure 10. When the bellows was pressurized to 1-1/2 times the design pressure those elements just beyond the start of the first convolution (locations J) were strained to the yield level, which was further verified by the fact that upon release of pressure, the gages at locations J showed residual tensile strains of ~ 2000 μin./in. All other operative gages returned to approximately zero. At the full design pressure, strain levels at location J would be less than one-third of the yield value. It should be noted that these pressurization tests were the only tests in which regions other than inside surfaces at convolution apexes (locations B) were the most highly strained elements in the bellows.

Maximum strains induced in the bellows by pressurization were computed using equations developed in the Appendix. The same assumptions were made as for extension equations. Consistent with the assumption that no interaction occurred between plies, it can also be assumed that each ply carried one-half the total pressure load. The effect of the equalizing ring tended to fix the convolution somewhere between the apex and the beginning of the straight portion. To obtain limiting values of the maximum strain it was assumed that the convolution was fixed first at the apex and secondly at the beginning of the straight portion. Considering the convolution fixed at the apex,

$$\epsilon = \frac{6p}{Et^2} K_1 + \frac{p}{Et} P_1 \qquad \text{(corresponds to Equation 19b in Appendix A)}$$

Substituting appropriate constants for the bellows and using a room temperature value for E,

$$\epsilon = 7.8\ p\ \mu\text{in./in.}$$

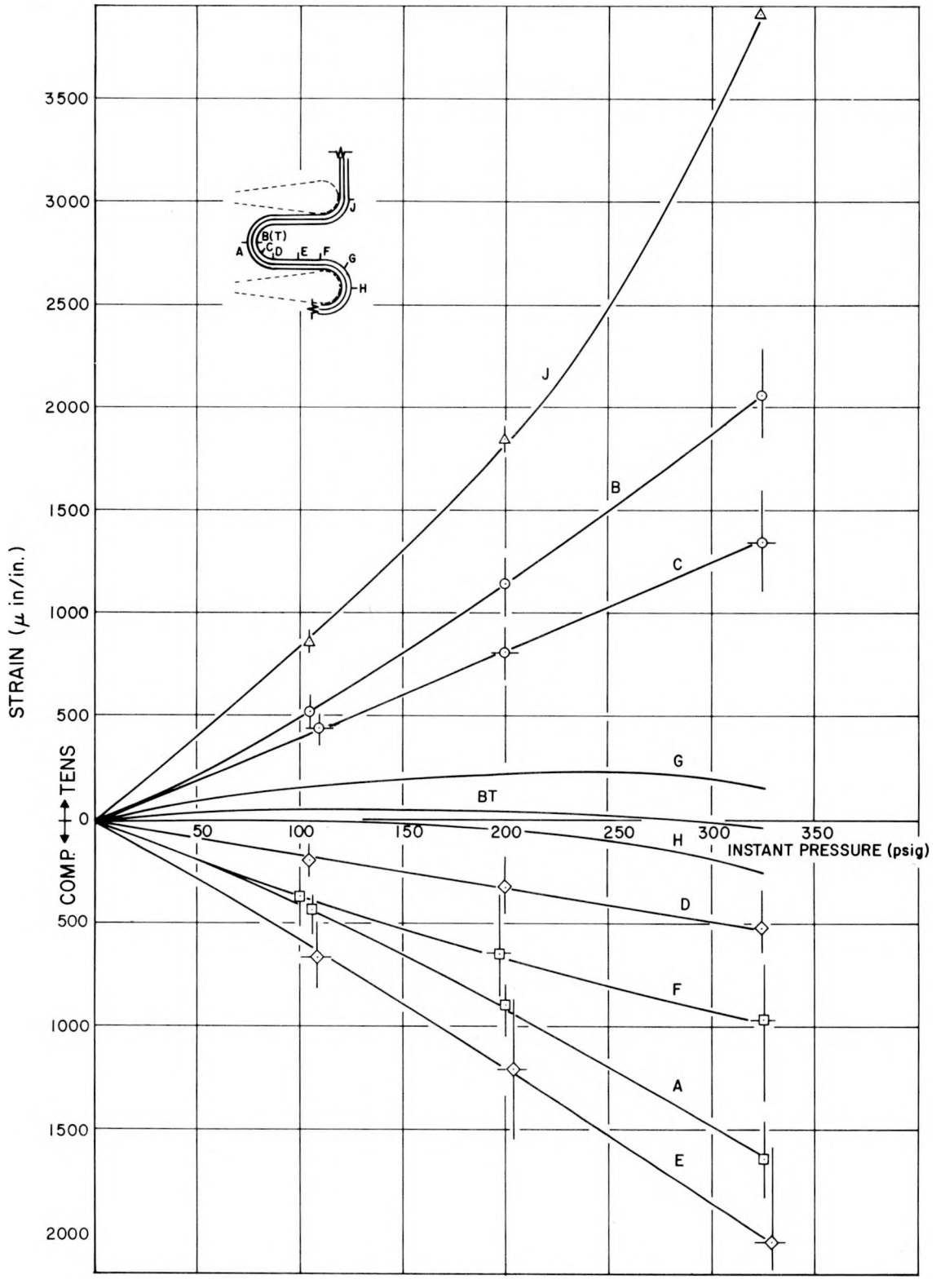

Figure 10. Strain vs Internal Pressure for Bellows at Room Temperature

Considering the convolution fixed at the beginning of the straight portion,

$$\epsilon = \frac{6p}{Et^2} K_2 + \frac{p}{Et} P_2$$ (corresponds to Equation 22b in Appendix A.

Substituting appropriate constants,

$$\epsilon = 3.42\ p\ \mu\text{in./in.}$$

Comparison of the experimental and theoretical curves (Figure 11) indicates that the test results are approximately half way between the two theoretical curves; this can be attributed to the interaction of the plies and to the unknown location of the point of fixity between the apex and the straight portion of the convolution. Therefore, using the theory which fixes the convolution at the beginning of the apex gives conservative (i.e., higher strain) results.

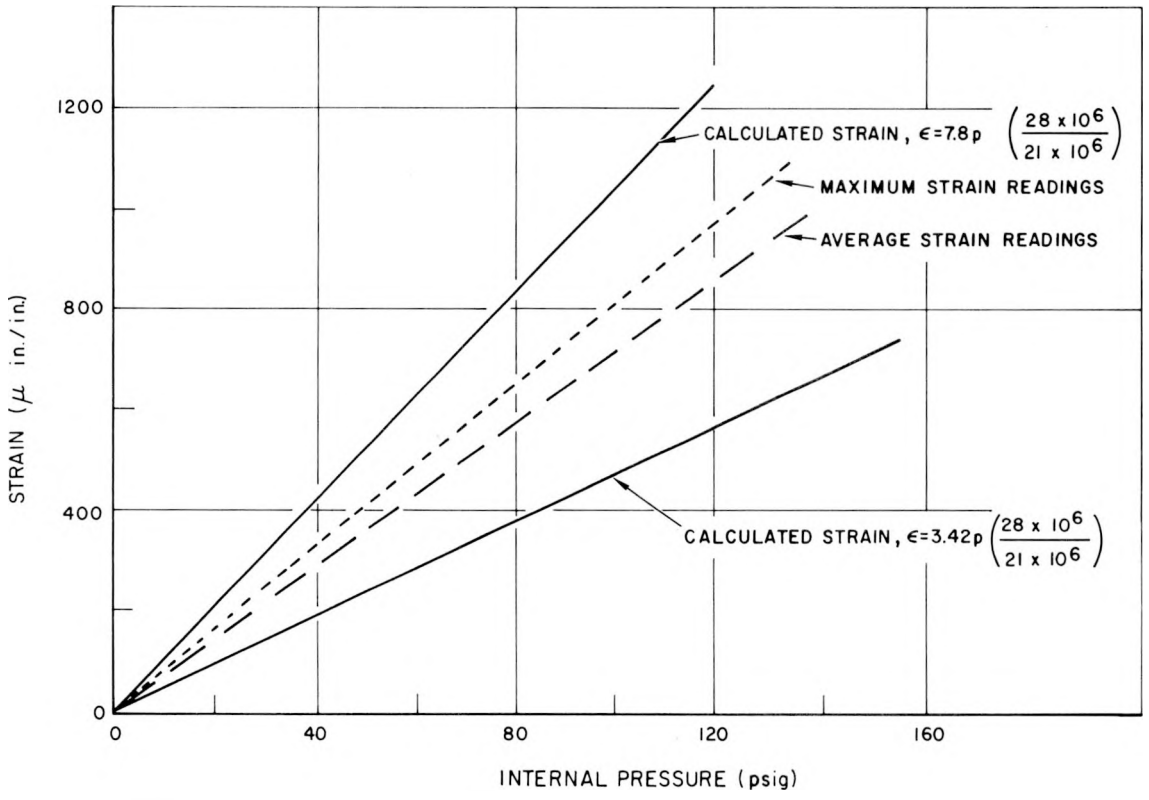

Figure 11. Comparison of Theoretical and Experimental Data for Internal Pressurization

E. ANGULAR ROTATION

The upper end of the bellows was tilted with relation to the bottom end from 0.1° to as high as 0.8°; this required a maximum end moment of 17,000 lb-ft. Once again the deformation was accomplished in steps, with a return to zero conditions after each step. Strain and deflection data were recorded throughout. Results from this series of tests did not follow a consistent pattern as in previous tests. This was not surprising as an unavoidable consequence of end tilting of the bellows was a simultaneous lateral displacement of the upper portion of the bellows of approximately 1/4 in. (due to the moment arm between the hinge and the top convolution); the combined effect of these deformations altered the strain pattern.

At the inside of one convolution apex (location B), a compressive strain of 1000 μin./in. was recorded. Adjacent to this point, at location C, a value of 925 μin./in., compression, was recorded. Elsewhere in the bellows the strains were substantially lower. Data from the three strain rosettes at locations A indicated that principal strains were essentially parallel to the longitudinal axis of the bellows. Upon release of loads all strain readings returned to approximately zero.

F. LATERAL DEFLECTION TESTS

A maximum side force of 42,500 lb was imposed upon the top of the bellows which resulted in a lateral deflection at the top face of 0.10 in. Loading was performed in successive steps (resulting in successive deflections of 0.01 in., 0.03 in., and 0.10 in.), with a return to zero after each step. The unit was prevented from tilting by the cross-arm members; therefore, a much smaller lateral deflection resulted from a substantially larger loading than in the previous angular rotation test series. Strain readings at locations B, for the top and bottom convolutions only, were as high as 800 μin./in., compression. Elsewhere values were significantly lower, and again the strain pattern was irregular. Upon release of load the strain readings returned to approximately zero.

G. TORSIONAL ROTATION TESTS

The resistance of the bellows to torsional rotation was very high, as might be expected for a structural component of such large diameter; the test-fixture columns deflected considerably more while reacting the torque than did the

bellows. Under an axial torque of 75,000 lb-ft, the top of the bellows rotated only 0.02° relative to the bottom. Recorded strains in the bellows all were less than 300 μin./in. during these tests, including those data from strain rosettes. Again upon release of load, strain values returned to zero.

There was some question as to the additional resistance to axial twisting provided by the linkages connecting the equalizing rings; therefore, these linkages were removed, and the bellows was twisted as before. The unit behaved essentially the same without the linkages as when they were attached (i.e., the amount of rotation and strain levels were the same as before). In an axial extension test with the linkages removed, strains and load-elongation characteristics also were the same as when linkages were in place.

H. COMBINED LOADING TESTS

In the final test series at room temperature, the bellows was subjected to all the foregoing modes of loading and deformation simultaneously. This was done by adding one mode of loading or deformation at a time until all modes were imposed. The order of imposition of modes and the resulting magnitude of load and deformation were:

TABLE II

COMBINED LOADS AND DEFORMATIONS APPLIED AT ROOM TEMPERATURE

Order	Mode	Load	Deformation
1	Axial Twisting	76,000 lb-ft	0.02°
2	Lateral Deflection	20,200 lb	0.07 in.
3	End Tilting	2,880 lb-ft	0.3°
4	Axial Extension	---	0.85 in.
5	Internal Pressurizing	210 psig	---

By following the above order the least severe loadings were imposed upon the bellows first. Pressurizing had to be done last because this required the use of special tension studs to react the axial load in excess of the normal test fixture capacity. These studs could be placed only after all deformations had been imposed upon the bellows. Also, it seemed probable that several interior strain gages would malfunction when again immersed in water, under pressure;

therefore, it was desirable to complete all other phases of the room-temperature testing program while these gages were still operative.

Strain data from this test series are summarized in Figure 12. On the basis of test data for the combined loads the following observations were made:

1) Torsional rotation, lateral deflection, and angular rotation of the magnitudes imposed did not cause a large proportion of the total strain induced in the bellows. Rosette data (from locations A) indicated that maximum principal strains were essentially parallel to the bellows axis throughout these tests.

2) Strains resulting from elongating and pressurizing the bellows caused a relatively large proportion of the total strain induced by the combined loading.

3) Strain patterns and magnitudes from single and combined mode tests generally were consistent; combined loading strains could be predicted approximately by superposition of strains from single mode tests. Location B was an exception as recorded extension strains were only half as large as expected.

4) During lateral deflection and angular rotation tests, the top and bottom convolutions of the bellows were strained more highly than the middle convolutions.

5) Axial extension of the bellows caused compressive circumferential strains at locations A (-400 to -900 μin./in. around the bellows periphery at 0.85 in. extension).

Some of the location B gages were behaving erratically during the elongation phase of combined loading tests; three of the six gages at this location appeared to be malfunctioning at this time, and none of the six were operable during the pressurization phase. Because of this uncertainty and inconsistencies between data from combined and single-mode loading tests (primarily for locations B), readings from location B taken during the elongation phase of combined tests were corrected by strain ratios obtained during single-mode testing.

For the pressurization phase, strain values again were estimated for locations B on the basis of ratios observed during the single mode testing. Average corrections and estimates are represented in Figure 12 by a dashed

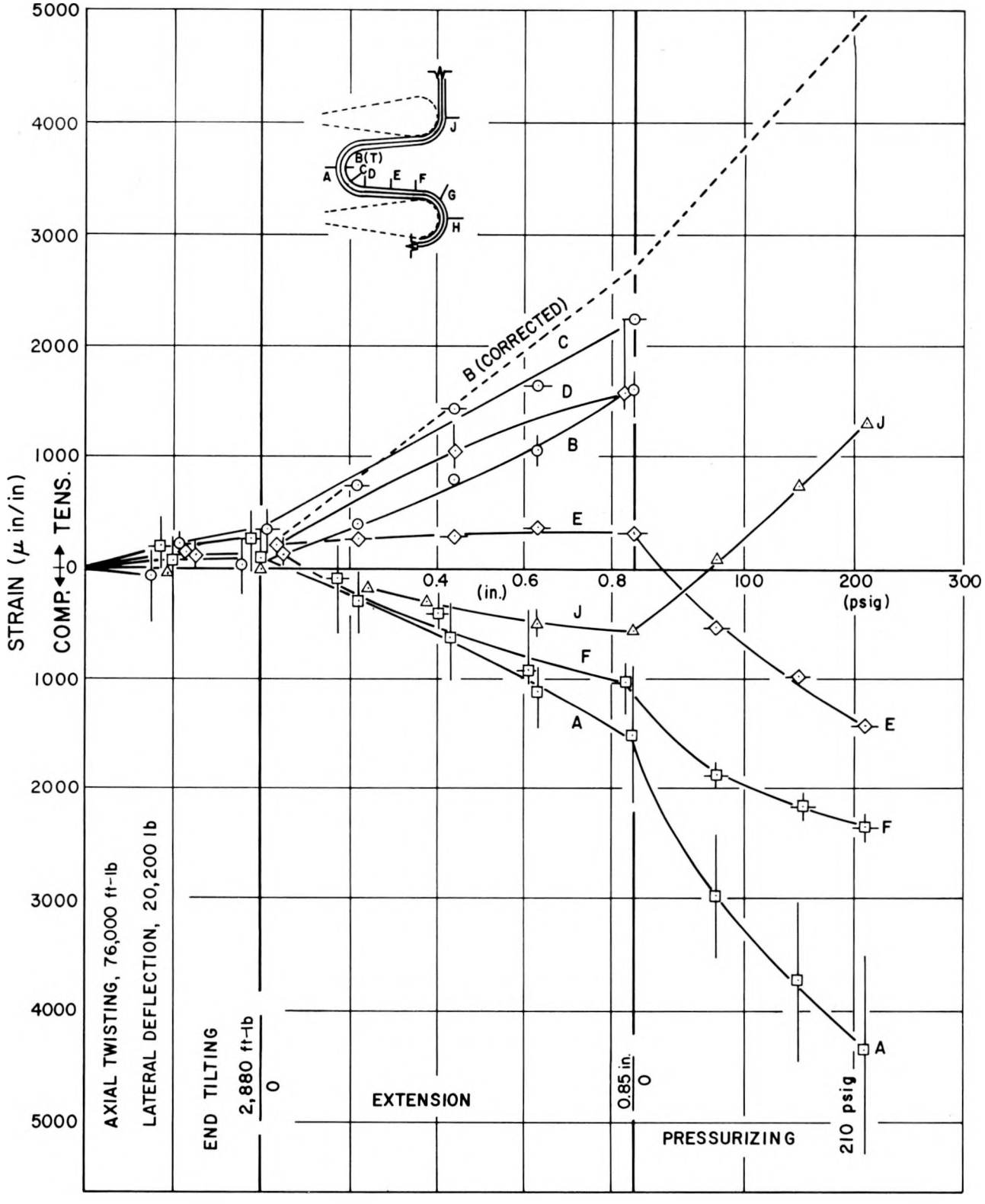

Figure 12. Strain vs Combined Load for Bellows at Room Temperature

curve. Although strain readings from locations A were somewhat higher than expected (on the basis of single-mode pressurization tests), these gages, which were mounted on the exterior surface of the bellows, were thought to be more reliable than those mounted on interior surfaces, as the latter were immersed in water during pressurization tests. Therefore, final estimates of maximum strain values were based primarily upon readings from locations A. These values were 3500 - 5000 μin./in., compression, at outside convolution apexes (locations A), and 4000 - 6000 μin./in., tension, at inside apexes (locations B). Variations between data from similar locations were attributed primarily to interaction effects.

V. HIGH TEMPERATURE TESTING PROGRAM

A. SIMULATION OF NORMAL REACTOR CONDITIONS

During normal reactor operation the intermediate-heat-exchanger bellows will be subjected to nominal extensions a great number of times while being pressurized internally. The first phase of the high temperature testing program was designed to simulate such typical operating conditions. However, extension values were increased beyond those expected during normal reactor service so that the number of cycles in this relatively short-term testing program would simulate the damage effect obtained during 20 years of normal reactor operation.

The bellows vessel was filled with sodium at 300°F, and the temperature of vessel and sodium were then brought to 1000°F. The unit was pressurized internally, in 15 psi steps, to 75 psig with a small quantity of nitrogen gas. Limit switches were set for an extension of 0.11 in. and the bellows was cycled 2155 times over a period of three days. (Some difficulty was encountered because of binding of the ball screw-and-nut assemblies.) These assemblies were the "dry" type, but operation was resumed without further difficulty only after the ball screws were oiled. During cycling the internal pressure of the bellows varied between 73 and 76 psig.

Efforts to measure strains induced in the bellows during this phase of testing were not successful; lead wires from the strain gages came in contact with the aluminum foil wrapping around the bellows and the gages shorted out. An estimate of the maximum strain values was made by superimposing pressure and extension strains from single mode tests, after making appropriate corrections to allow for temperature differences. Extension strains are not temperature dependent; therefore, values obtained at room temperature (see Figure 8) were utilized. For locations B, the imposed extension of 0.11 in. corresponded to 400 μin./in. tension. The equation for equality of loading-to-resistance ratio, p/E, at room and elevated temperatures was used to determine the strain component due to pressure, wherein,

$$\left(\frac{P}{E}\right)_{RT} = \left(\frac{P}{E}\right)_{1000},$$

where

P_{1000} = 75 psig (internal pressure at 1000°C)

E_{1000} = 21 x 10^6 psi (elastic modulus of Type 304 stainless steel at 1000°F)

E_{RT} = 28 x 10^6 psi (elastic modulus of Type 304 stainless steel at room temperature)

$P_{RT} = P_{1000} (E_{RT}/E_{1000}) = 75 (28/21) = 100$ psig,

which corresponded to a strain of 500 μin./in., tension (Figure 10). The estimate of maximum strain was obtained by summing the two strains, giving 900 μin./in., tension, at locations B.

At the conclusion of this test the space between plies of the bellows was pressurized with helium at 50 psig; no leaking was apparent in either ply, as evidenced by the fact that gas pressure remained at 50 psig for ~ 48 hours.

B. SIMULATION OF ABNORMAL REACTOR CONDITIONS

One of the most severe conditions foreseeable for the bellows during reactor operation would result from stoppage of the secondary pump in the heat exchanger system while the primary pump continued to operate. In the second phase of elevated temperature testing the resulting deformation effect of this situation was simulated; the number of elongation cycles was increased tenfold over that specified in the design criteria. With sodium at 1000°F and 5 psig inside the bellows, the unit was cycled 50 times over an extension range of 0.346 in. The pressure varied between 2 and 5 psig during cycling; the test was completed in ~ 1 hour.

From Figure 8 it was estimated that the maximum strain in the bellows was 1300 μin./in. tension, again at locations B. The amount of strain caused by internal pressure was negligible.

The space between plies was again pressurized with helium at 50 psig. The pressure did not drop over a period of several days, again indicating that there was no leaking in either ply of the bellows. Sodium was transferred to the storage tank at the conclusion of this test.

An even more severe condition for the bellows would result from stoppage of the heat exchanger primary pump, while the secondary pump continued to operate. In such an event the bellows would cool very rapidly; resulting circumferential contraction would leave a gap of ~ 1/32 in. between the convolution roots and corresponding equalizing rings. These deformation effects were simulated during the third phase of elevated temperature testing.

The test bellows had been fabricated with split equalizing rings to facilitate repositioning of the rings. The linkages were removed, and the rings were repositioned to provide a gap around each convolution root. Some difficulty was encountered in obtaining a uniform gap because the fixed diameter of the rings resulted in a smaller gap at the end points; however, use of adjustable bolting connectors between segments of the rings made it possible to adjust the gap between 1/32 to 1/8 in. The linkages used to connect equalizing rings had become warped during the preceding tests at elevated temperature; repair, and replacement of some studs was required. Therefore, it was decided to conduct this particular test series without the linkages in place, permitting repairs to be made in time for later tests.

After the rings were positioned, sodium at 300°F was transferred into the bellows vessel, and the vessel was heated to 800°F. During the period of heating, two audible thumps were noted which were attributed to adjustment of test fixtures due to differential extension; after completion of the test it was found that faulty welds on two of the equalizing-ring bolting brackets had failed, thus releasing the two bottom rings.

This test was conducted with sodium at 800°F and 75 psig inside the bellows; the pressure varied from 70 to 78 psig during cycling. The unit was cycled 50 times by extending it from the free position over an extension range of 0.38 in. A cycle period of ~ 3 min was used to permit recording of strain data at zero and fully extended conditions.

Three axial strain gages, located at the apexes of the two intermediate convolutions, gave readings of 800 ± 300 μin./ in., compression, at maximum elongation, over the duration of cycling. The fact that two of the equalizing rings were not secured during this test did not seem to influence the readings of those gages on the corresponding convolutions; this indicated that the convolutions deflected equally with or without the equalizing rings. Strains of

350 ± 200 μin./in., compression, were recorded at these same locations when the bellows was initially pressurized. Therefore, by summation the average total strain at locations A was 1150 ± 500 μin./in., compression, during this phase of testing.

An estimate was made of the strain at locations A, on the basis of single-mode test data, as a check on the above experimental data. A strain of 750 μin./in., compression, was obtained from Figure 10 for an extension of 0.380 in. Using the ratio, p/E, and the following values:

$$p_{800} = 75 \text{ psig}$$
$$E_{800} = 22 \times 10^6 \text{ psi}$$
$$E_{RT} = 28 \times 10^6 \text{ psi}$$
$$p_{RT} = p_{800} (E_{RT}/E_{800}) = 75 (28/22) = 95 \text{ psig},$$

a strain of 400 μin./in., compression, was obtained from Figure 12. Therefore, the total strain at locations A was estimated at 1150 μin./in., compression, which agrees with recorded values.

As it was not possible to make strain measurements on interior surfaces of the bellows in the presence of liquid sodium, it was necessary to estimate values of maximum strain for locations B. The same procedure of summing single mode test data was used. The extension component was 1400 μin./in., tension (from Figure 8), and the pressurization component was 450 μin./in., tension (from Figure 10), for a total of 1850 μin./in., tension.

At the conclusion of this test the space between plies of the bellows was again pressurized to 50 psig with helium. After initial adjustments the pressure remained at this level for several days, indicating that no leaking had occurred in either ply of the bellows. Again sodium was transferred from the test unit to the storage tank to permit repositioning of the equalizing rings preparatory to conducting the final tests on the bellows.

As the bellows now had demonstrated that it would withstand the loads and deflections expected during both normal and abnormal reactor conditions, it was felt that additional information of value might be obtained by determining not only the conditions necessary to cause failure of the bellows but also the mode of failure.

C. ENDURANCE TESTS

In previous tests it had been found that extending the bellows caused relatively higher strains in elements of the unit than any of the other deformation or loading modes. Therefore, endurance tests to deliberately induce failure were comprised of cyclic extensions of the bellows a significant number of times over each of a series of increasing stroke lengths.

Throughout the endurance tests the unit was filled with sodium at 1000°F and 75 psig (nominally). Leak checks were performed after completion of each test series. The first extension in the endurance tests was 0.35 in., to which the bellows was subjected 2400 times. The extension range was then increased to 0.50 in., and the unit was cycled an additional 2000 times. The unit was next extended over a range of 0.70 in., and after 1600 cycles, heater malfunction caused a drop in sodium temperature to ~ 800°F. After 400 more cycles at 800°F, a sharp pressure rise was recorded in the leak detecting system between bellows plies; an effort was made during 170 additional cycles to reproduce this effect, but without success. Faulty heaters were replaced, and testing was resumed at 1000°F over a cycle length of 1.00 in. It was necessary to alternately compress and extend the bellows between limits 0.50 in. either way from its original free position to obtain the 1-in. range. The unit was subjected to 20 cycles, when another pressure increase occurred between the bellows plies. Inasmuch as this effect could not be reproduced after a few cycles, testing was resumed and an additional 2000 cycles were imposed upon the bellows. Sodium temperature was maintained at 1000°F, and pressure in the vessel ranged from 57 to 80 psig.

The unit was next cycled between 0.88 in. below and 0.70 in. above the original free position; this provided a total stroke of 1.58 in. Pressure in the vessel varied from 52 to 82 psig. After 2350 cycles another sharp pressure rise occurred in the leak detection system; this was accompanied by actuation of the alarm system, which indicated that sodium had actually filled the space between bellows plies and overflowed into the attached well.

At this point, after accumulation of over 13,000 axial deflection cycles in sodium at 1000°F, testing was stopped; the vessel was emptied of sodium and permitted to cool. There was no evidence of leaking in the outer ply of the unit. This finding was consistent with the prediction, based upon room temperature tests, that failure would occur first in the inner ply at the apex of a convolution.

No strain data were obtained during endurance testing, as all gage installations had become inoperative due primarily to lead wire damage. Estimates were made of maximum strains (for locations B); these are included in Table III, which is a summary of maximum strains for all tests.

D. CUMULATIVE FATIGUE EFFECTS

The concept of "cumulative fatigue" has been evolved to take into account situations wherein load and deformation levels vary during the service history of a structure. According to this concept, the material in the structure changes as a result of the cyclic loading; changes of a detrimental nature are described as "damage" and these damage effects can accumulate.[2] At any given time in the service history the material has accumulated a certain level or degree of damage which may be related to a "cumulative damage factor". Theoretically, when this term exceeds 1.0 the material will fail.

Using the design fatigue curve given in Figure 13a and strain data from the tests on the bellows, a damage factor was calculated for each individual phase of the test. The damage factor for the 0.695-in. high-temperature extension test will be calculated as a typical example of the method used. The following test data are required:

$\Delta\epsilon$ = strain increment = 2860 μ in./in.

n = number of cycles = 1950.

According to Langer's method[1] when the alternating stress exceeds the yield stress of a material, the alternating stress for that cycle is equal to one-half of the stress range based on elastic theory. Considering strain instead of stress, the effective alternating strain is,

$$\epsilon_a = \frac{\Delta\epsilon}{2} = 1430\ \mu\text{in./in.}$$

Projecting the value of 1430 μin./in. on Figure 13a, it is determined that the number of cycles, N, which constitutes the design limitation, is 10,000.

TABLE III
SUMMARY OF DEFORMATIONS, LOADS, AND MAXIMUM STRAINS IMPOSED UPON THE HNPF IHX BELLOWS

Mode	Deformation	Load	ϵ^* (μin./in.)	Times	Temperature	Remarks
Axial Compression	0.5 in.	≈14,500 lb	-2000	1	room	Shipping condition
Axial Extension	0.25-0.58 in.	≈7,000-17,000 lb	900-2100	80	room	Positioning, static testing
Angular Rotation	0.1° 0.03 in.†	≈2,100 lb-ft	<300	2	room	
Angular Rotation	0.6° 0.19 in.†	≈13,000 lb-ft	-800	2	room	
Angular Rotation	0.8° 0.25 in.†	17,000 lb-ft	-1000	2	room	
Lateral Deflection	0.01 in.	≈4,200 lb	<300	3	room	Simulating service
Lateral Deflection	0.03 in.	≈13,000 lb	<300	3	room	deformations, separate
Lateral Deflection	0.10 in.	42,500 lb	-800	1	room	tests
Torsional Rotation	0.01°	38,000 lb-ft	300	3	room	
Torsional Rotation	0.02°	75,000 lb-ft	<300	8	room	
Internal Pressurizing	--	210 psig	1100	1	room (H_2O)	
Internal Pressurizing	--	325 psig	2100	1	room (H_2O)	
Torsional Rotation	0.02°	75,000 lb-ft				
Lateral Deflection	0.07 in.	20,200 lb-ft				Simulating service
End Tilting	0.3°	2,880 lb-ft	4000-6000	1	room	deformations, combined
Axial Extension	0.85 in.	--				testing
Internal Pressurizing	--	210 psig				
Axial Extension	0.11 in.	73-76 psig§	900	2155	1000°F (Na)	Normal reactor conditions
Axial Extension	0.35 in.	2-5 psig§	1300	50	1000°F (Na)	Abnormal reactor conditions
Axial Extension	0.52 in.	40 psig§	2100	1	1000°F (Na)	(Control malfunction)
Axial Extension	0.38 in.	70-78 psig§	1850	50	800°F (Na)	Abnormal reactor conditions, equalizing rings backed off 1/32 to 1/8 in.
Axial Extension	0.35 in.	72-78 psig§	1800	2400	1000°F (Na)	Endurance testing
Axial Extension	0.50 in.	68-80 psig§	2300	2000	1000°F (Na)	Endurance testing
Axial Extension	0.70 in.	62-77 psig§	3100	1600	1000°F (Na)	Endurance testing
Axial Extension	0.70 in.	62-77 psig§	3100	400	800°F (Na)	Endurance testing, pressure rise between plies
Axial Extension	0.70 in.	62-77 psig§	3100	170	800°F (Na)	Endurance testing
Axial Extension and Compression	1.00 in. $^{+0.50}_{-0.50}$	57-80 psig§	4150	20	1000°F (Na)	Endurance testing, pressure rise between plies
Axial Extension and Compression	1.00 in. $^{+0.50}_{-0.50}$	57-80 psig§	4150	2000	1000°F (Na)	Endurance testing
Axial Extension and Compression	1.58 in. $^{+0.70}_{-0.88}$	52-82 psig§	6500	2350	1000°F (Na)	Endurance testing, pressure rise between plies, sodium filled inter-ply well.

*At inside surface of convolution apex (location B), the most highly strained region.
† Lateral Deflection
§Internal pressure

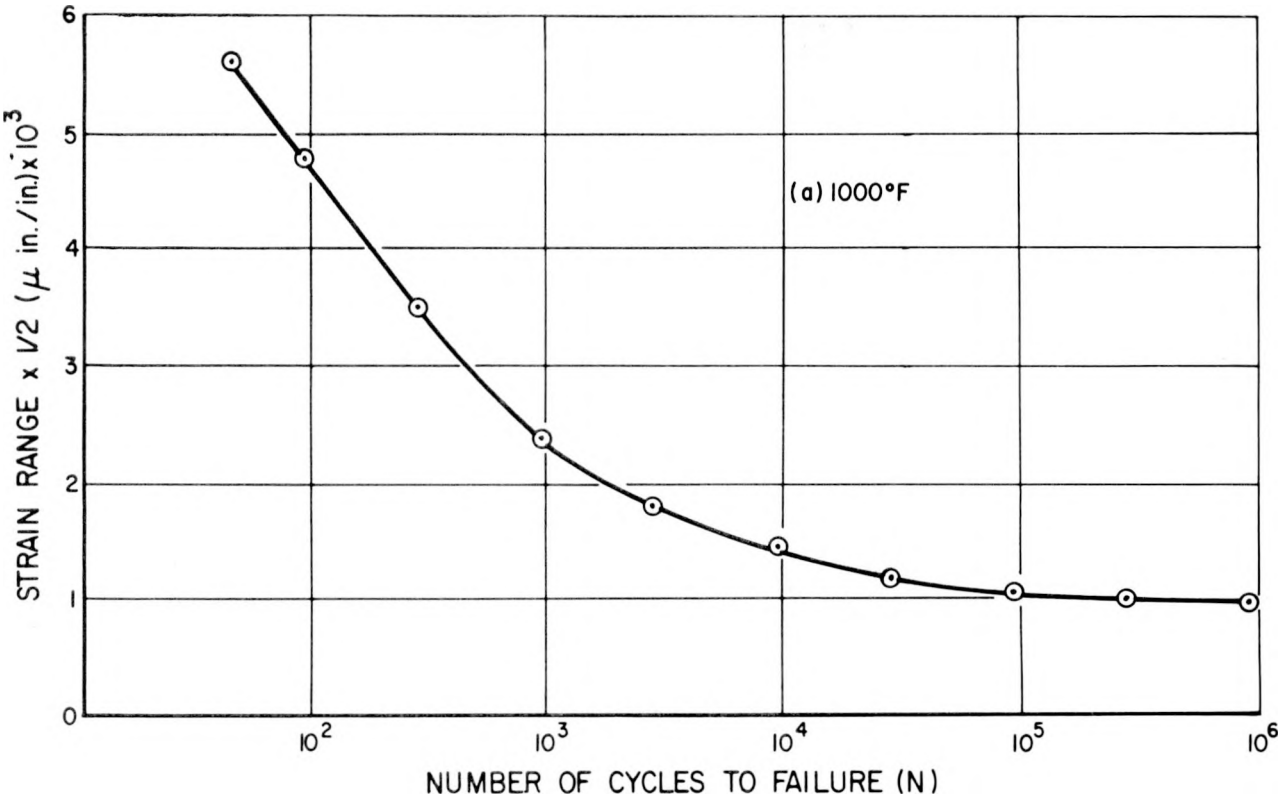

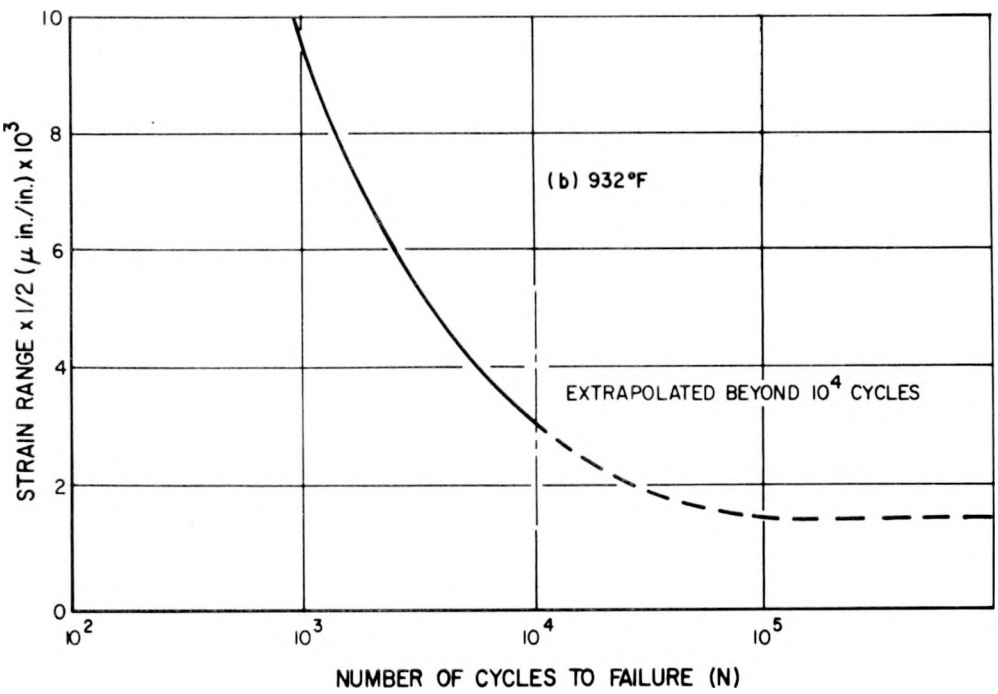

Figure 13. Strain-Fatigue Curves for Type 304 Stainless Steel at 930 to 1000°V

The number of test cycles, n, is 1950. The resultant damage factor, D', is given by:

$$D' = \frac{n}{N} = \frac{1950}{10,000} = 0.195 \quad .$$

The cumulative damage factor for all of the room temperature tests and all of the high temperature tests with an axial extension up to and including 0.495 in. was found to be less than 0.01. This means that during the normal service life of the bellows the cumulative damage effects will be almost negligible.

During the concluding portion of the test the bellows was deliberately cycled to failure. Table IV gives the cumulative damage factors for the final three portions of the test which applied the significant damage to the bellows. The damage factors given in Table IV are based on calculated strains using the methods derived in Appendix A and use the design fatigue curve (Figure 13a) as the failure criterion. From the information presented in Table IV, it can be seen that the cumulative damage factor for failure, based on the design fatigue curve, exceeds the theoretical value of 1.0.

TABLE IV

DAMAGE FACTORS BASED ON CALCULATED STRAINS

Total Displacement (in.)	Δp (psig)	n (cycles)	Strain (μin./in.)			Damage* Factor
			ϵ_δ	ϵ_p	ϵ_{tot}	
0.695	15	1950	2050	160	2210	0.043
1.00	23	2000	2950	240	3190	0.50
1.58	30	2400	4700	310	5010	2.93
					Cumulative Damage Factor	3.47

*Based on design fatigue curve (Figure 13a)

Tables V and VI list damage factors based on strains derived from the test data using actual strain-fatigue data[4] (Figure 13b) as the failure criterion. The cumulative damage factors given in Tables IV and V are significantly less than 1.0,

TABLE V

DAMAGE FACTORS BASED ON EXTRAPOLATED AVERAGE STRAIN DATA

Total Axial Deformation (in.)	Δp (psig)	n (cycles)	Strain (μin./in.)			Damage† Factor
			ϵ_{δ}*	ϵ_p	ϵ_{tot}	
0.695	15	1950	2500	110	2610	0.00
1.00	23	2000	3500	160	3710	0.057
1.58	30	2400	5600	220	5820	0.218
					Cumulative Damage Factor	0.28

*Extrapolated strain data
†Based on actual strain-fatigue curve (Figure13b)

TABLE VI

DAMAGE FACTORS BASED ON EXTRAPOLATED MAXIMUM STRAIN DATA

Total Displacement (in.)	Δp (psi)	n (cycles)	Strain (μin./in.)			Damage† Factor
			ϵ_{δ}*	ϵ_p	ϵ_{tot}	
0.695	15	1950	2750	120	2870	0.00
1.00	23	2000	3950	190	4140	0.080
1.58	30	2400	6250	240	6490	0.267
					Cumulative Damage Factor	0.35

*Extrapolated strain data
†Based on actual strain-fatigue curve (Figure 13b)

which tends to indicate the presence of a strain concentration. It is not unreasonable to expect a significant strain concentration factor since strains in the highly

stressed regions far exceed the material yield point. Applying a strain concentration factor of 1.7 to the strain data given in Tables V and VI results in cumulative damage factors of 0.935 and 1.157 for the average and maximum strain conditions respectively.

Langer[1] has indicated that in actual practice the calculated cumulative damage factor at failure may vary from 0.6 to 5.0 depending on the sequence of loading. If the lower stresses are applied first, followed by progressively higher stresses, the calculated value for the cumulative damage factor may be as high as 5.0. However, if the most damaging stresses are applied first for a significant number of cycles, failure can occur at a cumulative damage factor as low as 0.6.

From Figure 13a, it can be seen that the damage factor is very sensitive to changes in strain level. For instance, using a strain range of 1750 μ in./in., a 20% increase in strain will double the damage factor. Thus it is not surprising that, in practice, failure of the material does not occur exactly at the theoretical value of 1.0 for the cumulative damage factor. The damage factor value of 3.47 was obtained using *calculated* strains and the *design* fatigue curve. This value is raised above that normally expected primarily because the design fatigue-strength curve includes a factor of safety of 10 on the number of cycles and 1.5 on stress, and secondarily because the calculated strains are on the conservative side.

The cumulative damage factor of 0.3 was obtained using *actual* (i.e., experimentally observed) strains and *actual* strain-fatigue data. Thus, all the built-in conservatism discussed above has been removed. The fact that the damage factor falls *below* 1.0 is attributed to a strain concentration somewhere in the bellows. Such a strain concentration could be induced by a defect (e.g. variation in wall thickness, weld defect, pitting) covering an extremely small region.

When allowance is made for some of the factors discussed above, the values for cumulative damage factor obtained in these bellows tests are considered to be in good agreement with the expected values.

E. POST-TESTING INSPECTION OF BELLOWS

A thorough examination of the bellows was undertaken to determine the nature and extent of failure. First, the exterior surface was cleaned and checked with dye penetrant; no cracks were found. The vessel was then removed from the test

fixture. As rapid oxidation of the sodium residue might cause discoloration of the interior walls and obscure any cracks, care was exercised to prevent air from entering the unit. A 3-ft hole was opened in the head at one end of the vessel to permit inspection of the interior of the bellows; throughout this cutting process an argon atmosphere was maintained inside the vessel.

Once opened, the inside of the vessel was quickly cleaned of sodium residue and a visual inspection was made of the bellows interior. One typical fatigue crack was readily visible at the apex of an end convolution; this crack was ~ 1-3/4 in. long. The inside of the bellows then was checked with dye penetrant. Three categories of cracks were observed: (1) two large cracks, 1 to 2 in. long, at the apex of an end convolution, (2) several cracks of medium size and length, at convolution apexes, and (3) many hairline cracks of varying lengths in the region of convolution apexes (see Figure 14).

Sections of the bellows containing typical cracks were removed for further inspection. Of the cracks studied, only the two largest went completely through the inner ply; smaller cracks were at the inner surface only. The inner surface of the outside ply was checked for cracks with dye penetrant and none were found. A very thin layer of sodium (0.001 to 0.002 in.) was found between plies; limited oxidation of this material was observed after section edges had been cleaned.

Unexpected surface defects were observed at the interface between plies when they were separated. Photo-micrographs of a section through opposed pits [Figure 15(a) section, (b) plan] show severely worked material at the edge of a pit and with an inclusion in the opposing side. Four large pits were measured, and depths ranged from just under 0.0005 to 0.0072 in. The majority of pits appeared to be ~ 0.0005 in. deep. These surface defects appear to have resulted from galling action during forming of the bellows, and possibly were aggravated by fretting during cycling. Such defects were found over all interface surfaces of both plies, except in the immediate vicinity of convolution apexes.

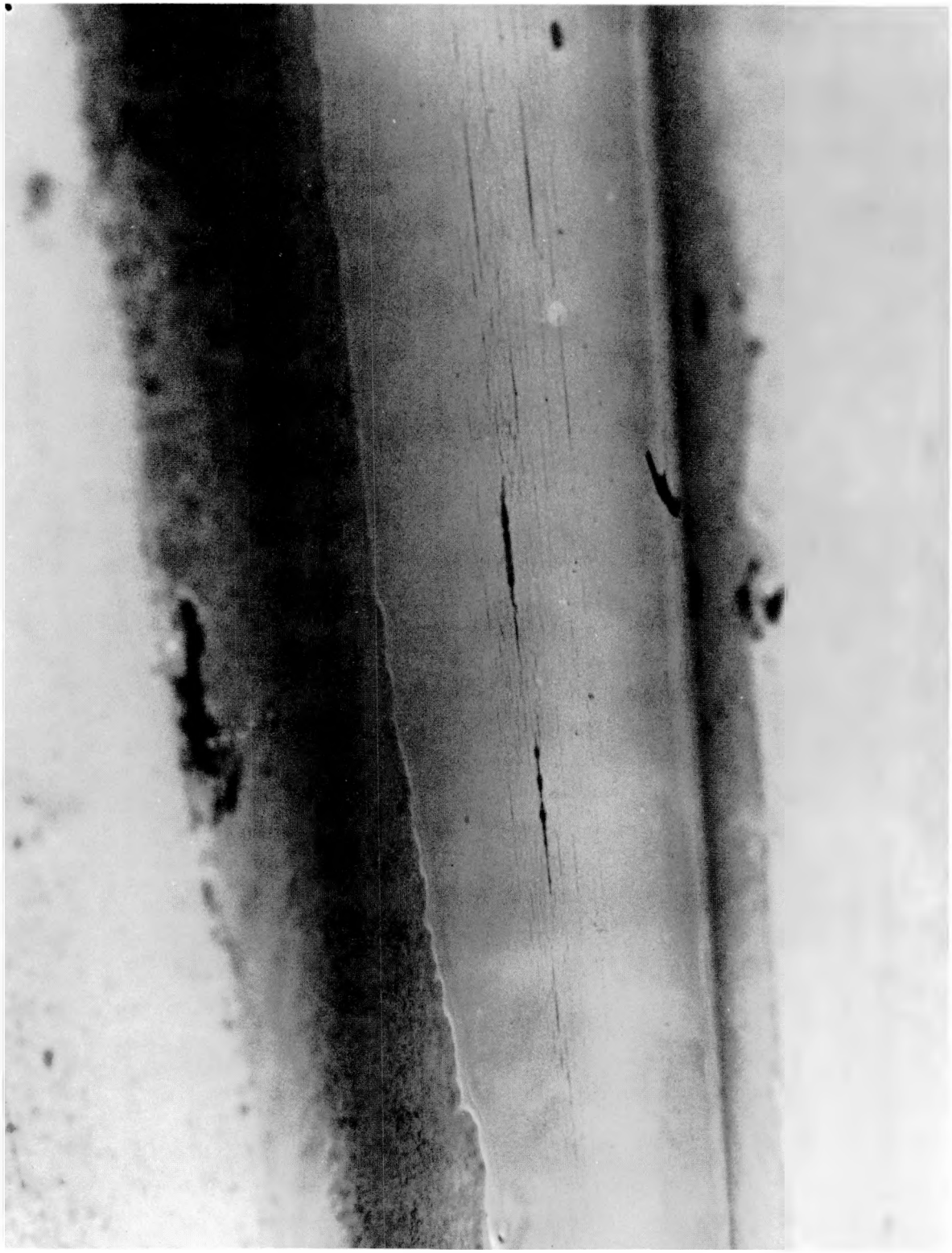

Figure 14. Fatigue Crack Pattern, Inner Ply of Bellows

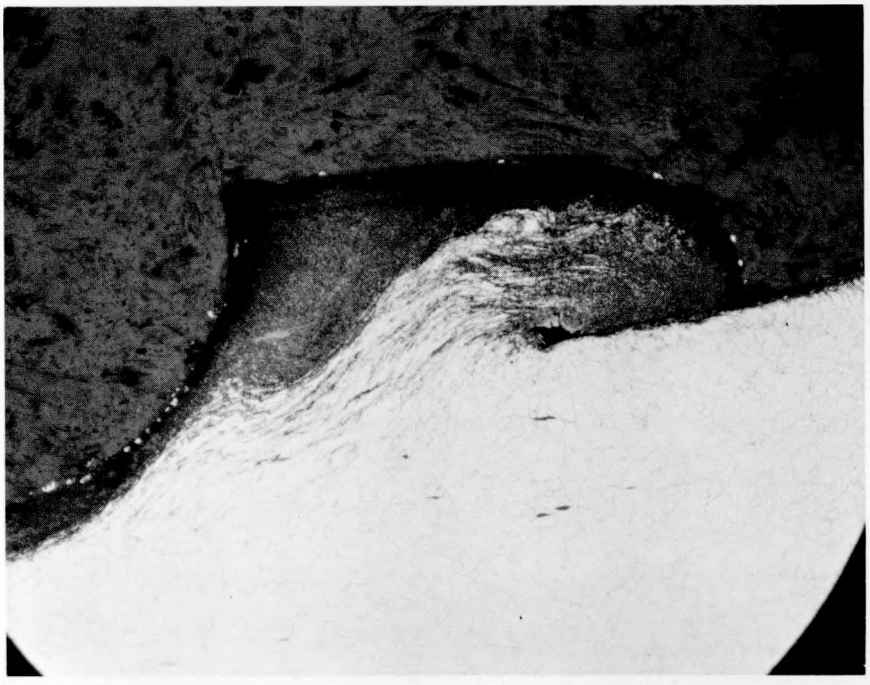

(a) Section Through Pit 175X

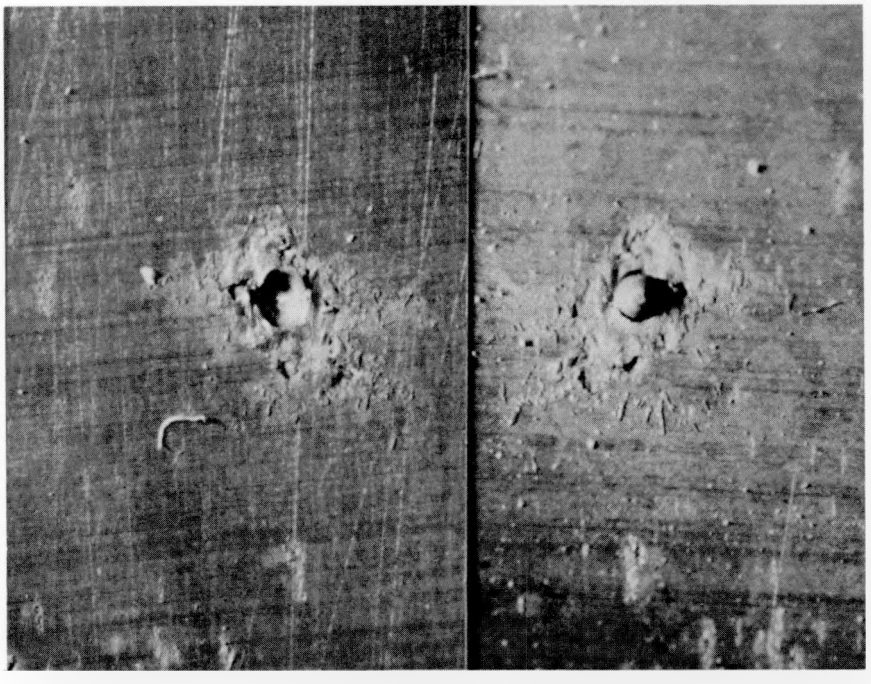

(b) Plan View Showing Pit and Inclusion 25X +

Figure 15. Pits at Interface of Plies

VI. SUMMARY

The results of this investigation demonstrate that the type of bellows tested is well suited for application in the HNPF intermediate heat exchanger.

The first phase of testing, conducted at room temperature, demonstrated that the analytical methods predicted stresses quite accurately and that stress levels were indeed low. Deformation and load limits for room-temperature axial deflection, pressurization, lateral deflection, angular rotation, and torsional rotation simulated the most severe conditions expected during reactor service. The most highly strained regions in the bellows were at inside surfaces of convolution apexes.

The second phase of testing, conducted with sodium at 75 psig and 1000°F inside the bellows, showed that negligible damage occurred during the simulated cycling effects of 20 years of normal reactor operation. The third phase of testing showed that the bellows could withstand the imposing of large strains during abnormal conditions involving failure of a pump in either the primary or secondary cooling system of the HNPF reactor.

During each of the preceding stages of testing, the loads and number of cycles were adjusted to simulate the damage effect of an order of magnitude more axial deflection cycles than would be expected during the life of the reactor. The cumulative damage factor resulting from all of the preceding tests was less than 0.01.

The fourth and final test was performed to deliberately induce failure of the bellows and showed that extremely large axial deflection (~60 times the normally expected deflection and 5 times the deflection following pump failure) were required to cause a reproducible leak indication. The leak occurred through the inner of the two bellows plies only; therefore, the structural integrity of the bellows was not breached and no sodium was lost from the system. Under reactor service conditions operation with the bellows could have continued until a leak developed in the outer ply.

The "cumulative damage factor" for the bellows approximated the theoretical value of 1.0 at the time a reproducible leak indication occurred. This value was obtained using experimental strain data, actual strain-fatigue data, and assuming a strain concentration factor of 1.7.

APPENDIX

DETERMINATION OF STRESSES IN AN EXPANSION JOINT WHEN SUBJECT TO PRESSURIZATION AND AXIAL DEFLECTION

In the case of the bellows expansion joint for the HNPF intermediate-heat-exchanger, the ratio of the maximum diameter to the minimum diameter is 1.0. When the ratio of the maximum to the minimum diameter approaches unity, as it does in this case, Timoshenko (Reference 3, page 68) states that the structure can be analyzed with sufficient accuracy by considering an elemental radial strip. Consequently, strip theory was used in this analysis to evaluate the stresses in the bellows when subjected to pressure loading and axial deflection.

1. Determination of Stresses Due to Axial Deflection

If a unit-width strip of the bellows is considered, then each half-convolution can be treated as a guided cantilever beam as shown in Figure 16.

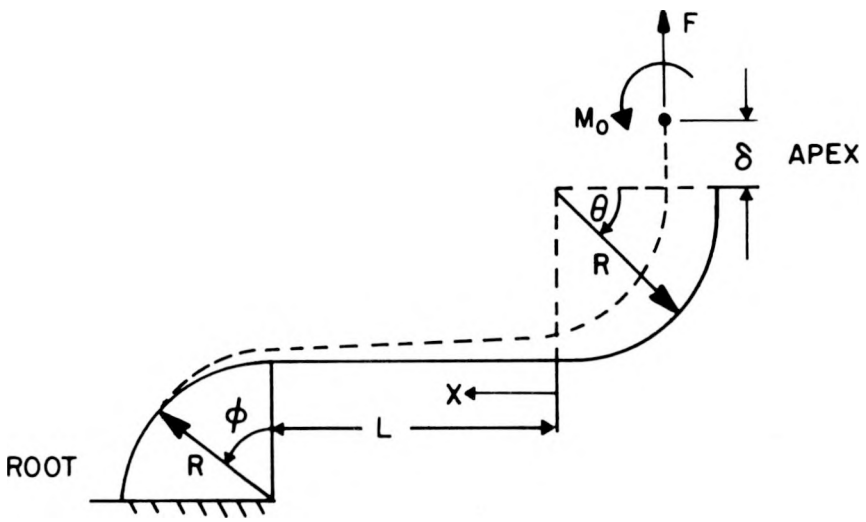

Figure 16. Half-Convolution as a Guided Cantilever Beam

Using energy relationships and applying Castigliano's theorem, the axial displacement can be found from the relationship,

$$\delta = \frac{\partial U}{\partial F} = \int \frac{M}{EI} \frac{\partial M}{\partial F} \, ds \, . \qquad \ldots(1)$$

Also, the rotation at the free end is defined as,

$$\psi = \frac{\partial U}{\partial M_o} = \int \frac{M}{EI} \frac{\partial M}{\partial M_o} ds \quad . \qquad \ldots (2)$$

For the case being considered, $\psi = 0$. For convenience, the moment M is separated into three parts, i.e.;

$$M_\theta = M_o + FR\,(1 - \cos\theta); \qquad 0 \leq \theta \leq \pi/2$$

$$M_x = M_o + FR + Fx; \qquad 0 \leq x \leq L$$

$$M_\phi = M_o + F(R + L) + FR \sin\phi; \qquad 0 \leq \phi \leq \pi/2.$$

Considering EI to be a constant and substituting the above values of M into Equations 1 and 2 result in the following:

$$EI\,\delta = \int_o^{\pi/2} \left[M_o + FR(1 - \cos\theta)\right](1 - \cos\theta)R^2 d\theta + \int_o^{L} (M_o + FR + Fx)(R + x)dx + \int_o^{\pi/2} \left[M_o + F(R + L) + FR\sin\phi\right]\left[(R + L) + R\sin\phi\right]Rd\phi \ , \qquad \ldots (3)$$

and

$$0 = \int_o^{\pi/2} \left[M_o + FR(1 - \cos\theta)\right]Rd\theta + \int_o^{L} (M_o + FR + Fx)dx + \int_o^{\pi/2} \left[M_o + F(R + L) + FR\sin\phi\right]Rd\phi \quad . \qquad \ldots (4)$$

Solving Equation 4 for F,

$$F = \frac{-2M_o}{2R + L} \quad . \qquad \ldots (5)$$

After integration, Equation 3 reduces to,

$$EI\delta = M_o\left[\pi R^2 + RL\left(1 + \frac{\pi}{2}\right) + \frac{L^2}{2}\right] + F\left[R^3\left(\frac{3\pi}{2}\right) + R^2L(3 + \pi) + RL^2\left(1 + \frac{\pi}{2}\right) + \frac{L^3}{12}\right] . \quad \ldots(6)$$

Substituting Equation 5 into Equation 6,

$$\frac{EI\delta}{M_o L^2} = -\frac{\frac{\pi}{2}\left(\frac{R}{L}\right)^3 + 2\left(\frac{R}{L}\right)^2 + \frac{\pi}{4}\left(\frac{R}{L}\right) + \frac{1}{12}}{\frac{R}{L} + \frac{1}{2}} . \quad \ldots(7)$$

Solving Equation 7 for M_o and setting,

$$C_1 = \frac{\frac{1}{L^2}\left(\frac{R}{L} + \frac{1}{2}\right)}{\frac{\pi}{2}\left(\frac{R}{L}\right)^3 + 2\left(\frac{R}{L}\right)^2 + \frac{\pi}{4}\left(\frac{R}{L}\right) + \frac{1}{12}}$$

$$= \frac{1}{L^2}\,\frac{\left(\frac{R}{L}\right) + 0.5}{1.57\left(\frac{R}{L}\right)^3 + 2\left(\frac{R}{L}\right)^2 + 0.785\left(\frac{R}{L}\right) + 0.0834} .$$

Therefore,

$$M_o = -EI\delta C_1 . \quad \ldots(8)$$

Since this analysis is based on strip theory, the maximum bending stress in the bellows due to an axial displacement is,

$$\sigma = \frac{M_o t}{2I} \quad \ldots(9a)$$

$$= \frac{Et\delta}{2} C_1 .$$

Note that in Equation 9a the minus sign has been dropped since it simply represents which side of the bellows is in tension or compression. In the case of a

bellows with S convolutions subjected to a displacement, d, the peak bending stress is,

$$\sigma = \frac{Etd}{4S} C_1 \quad . \qquad \ldots (9b)$$

In terms of strain, the above can be written as

$$\epsilon = \frac{td}{4S} C_1 \quad . \qquad \ldots (9c)$$

The maximum stress in the bellows is comprised of bending and axial components and is equal to,

$$\sigma_{max} = \frac{Etd}{4S} C_1 + \frac{F}{t} \ ,$$

or, substituting Equations 5, 8, and $\delta = \frac{d}{2S}$,

$$\sigma_{max} = \frac{Etd}{4S} C_1 \left[1 + \frac{t}{3(2R + L)}\right] \qquad \ldots (10a)$$

or in terms of strain,

$$\epsilon_{max} = \frac{td}{4S} C_1 \left[1 + \frac{t}{3(2R + L)}\right] \quad . \qquad \ldots (10b)$$

Since t is normally much smaller than either R or L, Equation 10a demonstrates that the direct stress component usually is small and can be disregarded.

If the convolution is considered fixed at the end of the flat portion of the bellows, as shown in Figure 17, Equations 3 and 4 are reduced to,

$$EI\delta = \int_o^{\pi/2} \left[M_o + FR(1 - \cos\theta)\right](1 - \cos\theta)R^2 d\theta + \int_o^L (M_o\, FR + Fx)(R + x)dx \quad , \qquad \ldots (11)$$

and

$$0 = \int_o^{\pi/2} \left[M_o + FR(1 - \cos\theta)\right]Rd\theta + \int_o^L (M_o + FR + Fx)dx \quad . \qquad \ldots (12)$$

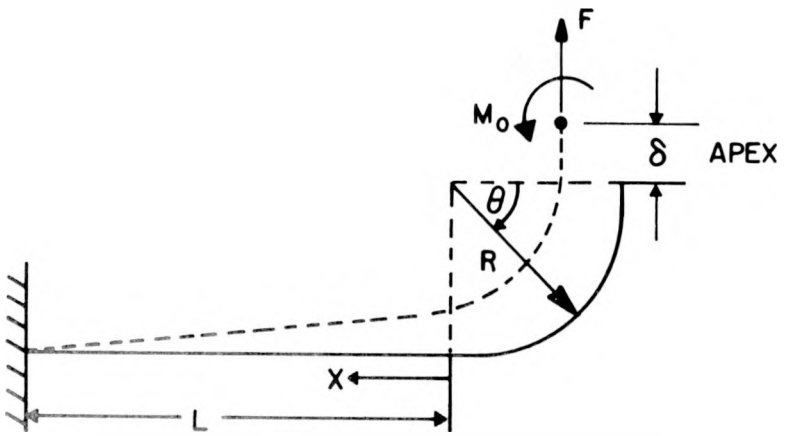

Figure 17. Convolution Fixed at Flat Portion of Bellows

Solutions of Equations 11 and 12 lead to a form similar to Equation 9b, except that C_1 is replaced by C_2,

$$\sigma = \frac{Etd}{4S} C_2 \quad , \qquad \ldots (13a)$$

or

$$\epsilon = \frac{td}{4S} C_2 \quad , \qquad \ldots (13b)$$

where

$$C_2 = \frac{\frac{1}{L^2}\left[\left(\frac{\pi}{2} - 1\right)\left(\frac{R}{L}\right)^2 + \left(\frac{R}{L}\right) + \frac{1}{2}\right]}{\left(\frac{\pi^2}{8} - 1\right)\left(\frac{R}{L}\right)^4 + \frac{\pi}{4}\left(\frac{R}{L}\right)^3 + \left(\frac{R}{L}\right)^2 + \frac{\pi}{6}\left(\frac{R}{L}\right) + \frac{1}{12}}$$

$$= \frac{1}{L^2} \; \frac{0.571\left(\frac{R}{L}\right)^2 + \left(\frac{R}{L}\right) + 0.5}{0.231\left(\frac{R}{L}\right)^4 + 0.785\left(\frac{R}{L}\right)^3 + \left(\frac{R}{L}\right)^2 + 0.524\left(\frac{R}{L}\right) + 0.0834} \; .$$

Since it has been demonstrated that the direct stress component is relatively small, Equation 13a can be used directly to obtain the maximum stress in the bellows.

2. Determination of Stresses Due to Pressurization

As in the previous case, a unit-width strip is considered as a guided cantilever beam, as shown in Figure 18.

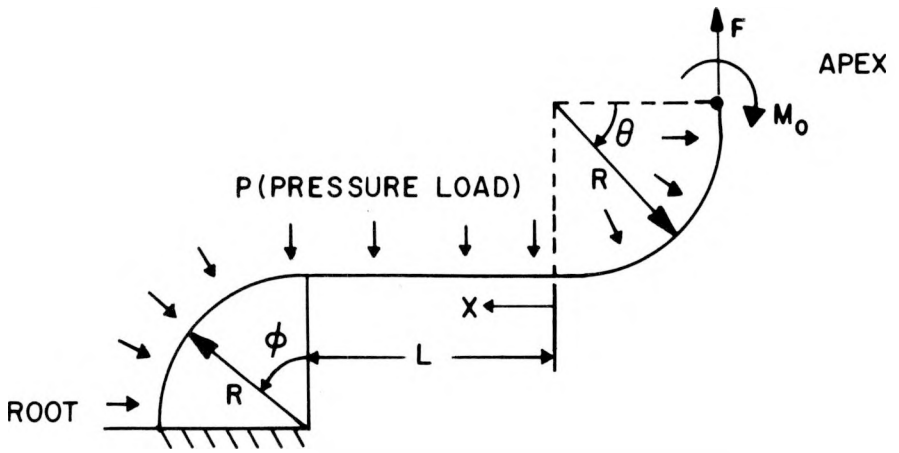

Figure 18. Unit-Width Strip Considered as a Guided Cantilever

The horizontal components of the pressure loading result in circumferential forces and do not affect the analysis of the elemental strip. From symmetry,

$$F = p\left(R + \frac{L}{2}\right) \quad . \qquad \ldots(14)$$

Using Equation 2 again and noting that for compatibility the rotation at the free end is zero,

$$\psi = \frac{\partial U}{\partial M_o} = \int \frac{M}{EI} \frac{\partial M}{\partial M_o} ds = 0 \quad . \qquad \ldots(15)$$

As was done previously, the moment M is separated into three parts; i.e.,

$$M_\theta = FR(1 - \cos\theta) - M_o - \frac{pR^2}{2}(1 - \cos\theta)^2 \qquad 0 \le \theta \le \frac{\pi}{2}$$

$$M_x = F(R + x) - M_o - \frac{p}{2}(R + x)^2 \qquad 0 \le x \le L$$

$$M_\phi = \left[F - p(R + L)\right]R \sin\phi - \frac{pR^2}{2}\sin^2\phi + F(R + L) - M_o - \frac{p}{2}(R + L)^2 \qquad 0 \le \phi \le \frac{\pi}{2} \quad .$$

Substituting the above values of M into Equation 15, and using the relationship given in Equation 14,

$$0 = \int_o^{\pi/2} \left[pR\left(R + \frac{L}{2}\right)(1 - \cos\theta) - M_o - \frac{pR^2}{2}(1 - \cos\theta)^2 \right] R d\theta$$

$$+ \int_o^{L} \left[p\left(R + \frac{L}{2}\right)(R + x) - M_o - \frac{p}{2}(R + x)^2 \right] dx$$

$$+ \int_o^{\pi/2} \left[-\frac{pRL}{2}\sin\phi - \frac{pR^2}{2}\sin^2\phi + p\left(R + \frac{L}{2}\right)(R + L) - M_o - \frac{p}{2}(R + L)^2 \right] R d\theta \quad . \qquad \ldots(16)$$

Solving Equation 16 for M_o,

$$M_o = pL^2 \frac{\frac{\pi}{4}\left(\frac{R}{L}\right)^3 + \frac{\pi - 1}{2}\left(\frac{R}{L}\right)^2 + \frac{1}{2}\left(\frac{R}{L}\right) + \frac{1}{12}}{\pi\left(\frac{R}{L}\right) + 1} \quad . \qquad \ldots(17a)$$

Let

$$K_1 = L^2 \frac{\frac{\pi}{4}\left(\frac{R}{L}\right)^3 + \frac{\pi - 1}{2}\left(\frac{R}{L}\right)^2 + \frac{1}{2}\left(\frac{R}{L}\right) + \frac{1}{12}}{\pi\left(\frac{R}{L}\right) + 1}$$

$$= L^2 \frac{0.785\left(\frac{R}{L}\right)^3 + 1.07\left(\frac{R}{L}\right)^2 + 0.5\left(\frac{R}{L}\right) + 0.0834}{3.14\left(\frac{R}{L}\right) + 1} \quad ,$$

Then,

$$M_o = pK_1 \quad . \qquad \ldots(17b)$$

The maximum bending stress in the bellows is,

$$\sigma = \frac{6M_o}{t^2} = \frac{6p}{t^2}K_1 \quad . \qquad \ldots(18)$$

The maximum stress in the bellows is the sum of the bending and normal components, or,

$$\sigma_{max} = \frac{6p}{t^2} K_1 + \frac{p}{t} P_1 \qquad \ldots (19a)$$

or in terms of strain

$$\epsilon_{max} = \frac{6p}{Et^2} K_1 + \frac{p}{Et} P_1 \qquad \ldots (19b)$$

where

$$P_1 = R + \frac{L}{2} \ .$$

Considering the convolution to be fixed at one end of the flat portion of the bellows, as shown in Figure 19, Equation 16 reduces to

$$0 = \int_o^{\pi/2} \left[FR(1 - \cos\theta) - M_o - \frac{pR^2}{2}(1 - \cos\theta)^2 \right] R d\theta$$

$$+ \int_o^{L} \left[F(R + x) - M_o - \frac{p}{2}(R + x)^2 \right] dx \ . \qquad \ldots (20)$$

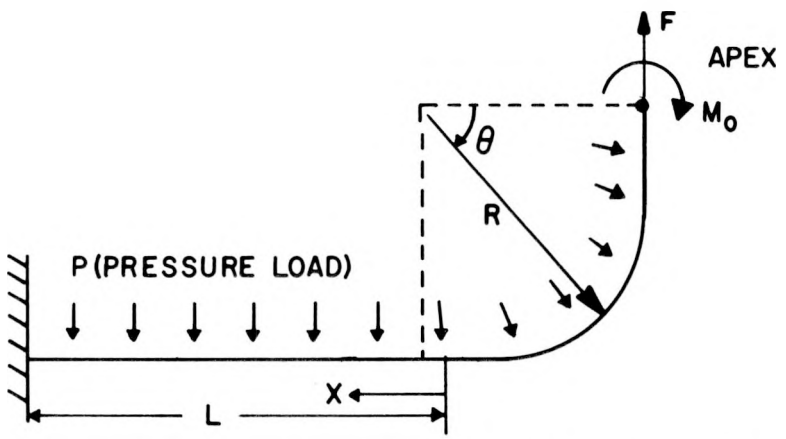

Figure 19. Convolution Fixed at One End of Flat Portion of Bellows

To find the force, F, the relationship given in Equation 1 is used. Substituting the values of M_θ and M_x on page 48 into Equation 1, and noting that the deflection, δ, is zero,

$$\delta = 0 = \int_o^{\pi/2} \left[FR(1 - \cos\theta) - M_o - \frac{pR^2}{2}(1 - \cos\theta)^2\right](1 - \cos\theta)R^2 d\theta$$

$$+ \int_o^{L} \left[F(R + x) - M_o - \frac{p}{2}(R + x)^2\right](R + x)dx \quad . \qquad \ldots (21)$$

Eliminating M_o from Equations 20 and 21 and solving for F,

$$F = pL \frac{\left(\frac{\pi^2}{8} - \frac{\pi}{24} - 1\right)\left(\frac{R}{L}\right)^5 + \left(\frac{\pi}{4} - \frac{1}{3}\right)\left(\frac{R}{L}\right)^4 + \left(1 - \frac{\pi}{16}\right)\left(\frac{R}{L}\right)^3 + \left(\frac{\pi + 1}{6}\right)\left(\frac{R}{L}\right)^2 + \left(\frac{\pi}{16} + \frac{1}{12}\right)\left(\frac{R}{L}\right) + \frac{1}{24}}{\left(\frac{\pi^2}{8} - 1\right)\left(\frac{R}{L}\right)^4 + \frac{\pi}{4}\left(\frac{R}{L}\right)^3 + \left(\frac{R}{L}\right)^2 + \frac{\pi}{6}\left(\frac{R}{L}\right) + \frac{1}{12}} .$$

Substituting the above value for F into Equation 20 and solving for M_o,

$$M_o = pL^2 \left[\left(\frac{\pi^3}{64} - \frac{\pi^2}{48} - \frac{\pi}{12}\right)\left(\frac{R}{L}\right)^7 + \left(\frac{3\pi^2}{32} - \frac{5\pi}{24} - \frac{1}{6}\right)\left(\frac{R}{L}\right)^6 + \left(\frac{7\pi}{24} - \frac{\pi^2}{32} - \frac{1}{3}\right)\left(\frac{R}{L}\right)^5\right.$$

$$+ \left(\frac{\pi}{48} + \frac{1}{3}\right)\left(\frac{R}{L}\right)^4 + \left(\frac{\pi^2}{32} - \frac{\pi}{16} + \frac{1}{6}\right)\left(\frac{R}{L}\right)^3 + \left(\frac{\pi}{12} - \frac{1}{12}\right)\left(\frac{R}{L}\right)^2$$

$$\left. + \left(\frac{1}{24} + \frac{\pi}{288}\right)\left(\frac{R}{L}\right) + \frac{1}{144}\right]\left\{1 \Big/ \left[\left(\frac{\pi^2}{8} - 1\right)\left(\frac{R}{L}\right)^4 + \frac{\pi}{4}\left(\frac{R}{L}\right)^3 + \left(\frac{R}{L}\right)^2 + \frac{\pi}{6}\left(\frac{R}{L}\right) + \frac{1}{12}\right]\left[\frac{\pi}{2}\left(\frac{R}{L}\right) + 1\right]\right\}.$$

The maximum stress at the apex of the bellows is

$$\sigma_{max} = \frac{6p}{t^2} K_2 + \frac{p}{t} P_2 \quad . \qquad \ldots (22a)$$

In terms of strain

$$\epsilon_{max} = \frac{6p}{Et^2} K_2 + \frac{p}{Et} P_2 \quad , \qquad \ldots (22b)$$

where

$$K_2 = L^2 \frac{0.017\left(\frac{R}{L}\right)^7 + 0.104\left(\frac{R}{L}\right)^6 + 0.275\left(\frac{R}{L}\right)^5 + 0.399\left(\frac{R}{L}\right)^4 + 0.279\left(\frac{R}{L}\right)^3 + 0.179\left(\frac{R}{L}\right)^2 + 0.0525\left(\frac{R}{L}\right) + 0.00694}{\left[0.231\left(\frac{R}{L}\right)^4 + 0.785\left(\frac{R}{L}\right)^3 + \left(\frac{R}{L}\right)^2 + 0.524\left(\frac{R}{L}\right) + 0.0834\right]\left[1.57\left(\frac{R}{L}\right) + 1\right]}$$

$$P_2 = L \frac{0.100\left(\frac{R}{L}\right)^5 + 0.452\left(\frac{R}{L}\right)^4 + 0.804\left(\frac{R}{L}\right)^3 + 0.691\left(\frac{R}{L}\right)^2 + 0.279\left(\frac{R}{L}\right) + 0.0416}{0.231\left(\frac{R}{L}\right)^4 + 0.785\left(\frac{R}{L}\right)^3 + \left(\frac{R}{L}\right)^2 + 0.524\left(\frac{R}{L}\right) + 0.0834} .$$

The maximum moment at the point of assumed fixity is,

$$M_r = M_o + \frac{p}{2}(R + L)^2 - F(R + L) . \qquad \ldots (23)$$

Consequently, the maximum stress at the point of assumed fixity

$$\sigma_{max} = \frac{6p}{t^2} K_2 + \frac{3p}{t^2}(R + L)^2 - \frac{6p}{t^2} P_2 (R + L) ,$$

or

$$\sigma_{max} = \frac{6p}{t^2}\left[K_2 + \frac{1}{2}(R + L)^2 - P_2 (R + L)\right] . \qquad \ldots (24a)$$

In terms of strain,

$$\epsilon_{max} = \frac{6p}{Et^2}\left[K_2 + \frac{1}{2}(R + L)^2 - P_2 (R + L)\right] . \qquad \ldots (24b)$$

NOMENCLATURE

Symbols

D = damage factor
d = axial displacement of bellows (in.)
ds = element of length (in.)
E = Young's Modulus (psi)
F = force (lb)
I = section moment of inertia per unit of width ($in.^4/in.$)
L = straight portion of convolution (in.)
M = bending moment per unit of width (in./lb-in.)
N = fatigue design limit
n = number of applied cycles
p = pressure (psi)
R = convolution radius (in.)
S = number of convolutions
t = material thickness (in.)
U = strain energy (in./lb)
ψ, θ, ϕ = angles
δ = deflection of one-half convolution (in.)
ϵ = strain (dimensionless)
σ = stress (psi)
C_1, C_2, K_1, K_2, P_1, P_2 = constants depending on convolution geometry
s = element of convolution length
x = variable distance

Subscripts

max refers to maximum value
o refers to initial condition
r refers to root condition
θ, x, ϕ refers to coordinate axis
δ refers to axial deflection test
p refers to pressurization test

REFERENCES

1. B. F. Langer, "Design Values of Thermal Stress in Ductile Material," WAPD-CTA (CE)-64 (May 15, 1957)
2. M. A. Miner, "Cumulative Damage in Fatigue," Journal of App. Mech., 1945; pp A159-A164
3. S. Timoshenko, Theory of Plates and Shells, (McGraw-Hill Book Co., Inc., New York, 1940)
4. A. Johansson, "Fatigue of Steels at Constant Strain Amplitude and Elevated Temperatures," Proceedings of Colloquim on Fatigue (Stockholm, 1955)